Bull Volcanol (2011) 73:373–394
DOI 10.1007/s00445-011-0449-0

RESEARCH ARTICLE

Geochemistry of volcanic and hydrothermal gases of Mutnovsky volcano, Kamchatka: evidence for mantle, slab and atmosphere contributions to fluids of a typical arc volcano

Mikhail Zelenski · Yuri Taran

Received: 3 August 2009 / Accepted: 11 December 2010 / Published online: 17 May 2011

Abstract We report chemical compositions (major and trace components including light hydrocarbons), hydrogen, oxygen, helium and nitrogen isotope ratios of volcanic and geothermal fluids of Mutnovsky volcano, Kamchatka. Several aspects of the geochemistry of fluids are discussed: chemical equilibria, mixing of fluids from different sources, evaluation of the parent magmatic gas composition and contributions to magmatic vapors of fluids from different reservoirs of the Kamchatkan subduction zone. Among reactive species, hydrogen and carbon monoxide in volcanic vapors are chemically equilibrated at temperatures >300°C with the SO_2-H_2S redox-pair. A metastable equilibrium between saturated and unsaturated light hydrocarbons is attained at close to discharge temperatures. Methane is disequilibrated. Three different sources of fluids from three fumarolic fields in the Mutnovsky craters can be distinguished: (1) magmatic gas from a large convecting magma body discharging through Active Funnel, a young crater with the hottest fumaroles (up to 620°C) contributing ~80% to the total volcanic gas output; (2) volcanic fluid from a separate shallow magma body beneath the Bottom Field of the main crater (96–280°C fumaroles); and (3) hydrothermal fluid with a high relative and absolute concentrations of CH_4 from the Upper Field in the main crater (96–285°C fumaroles). The composition of the parent magmatic gas is estimated using water isotopes and correlations between He and other components in the Active Funnel gases. The He-Ar-N_2 systematics of volcanic and hydrothermal fluids of Mutnovsky are consistent with a large slab-derived sedimentary nitrogen input for the nitrogen inventory, and we calculate that only ~1% of the magmatic N_2 has a mantle origin and <<1% is derived from the arc crust.

Keywords Volcanic gases · He and N isotopes · Subduction · Recycling · Hydrothermal systems

Editorial responsibility: S. Inguaggiato

This paper constitutes part of a special issue. The complete citation information is as follows:

Zelenski M, Taran Y (2011) Geochemistry of volcanic and hydrothermal gases of Mutnovsky volcano, Kamchatka: evidence for mantle, slab and atmosphere contributions to fluids of a typical arc volcano. In: Inguaggiato S, Shinohara H, and Fischer T (eds) Geochemistry of volcanic fluids: a special issue in honor of Yuri A. Taran. Bull Volcanol 73(4): 373–394

M. Zelenski
Institute of Experimental Mineralogy,
Chernogolovka,
Moscow District, Russia

Y. Taran (✉)
Institute of Geophysics,
Universidad Nacional Autónoma de México,
Mexico D.F. 04510, Mexico
e-mail: taran@geofisica.unam.mx

Introduction

Degassing of volatiles through active arc volcanoes is a direct manifestation and a measureable property of the volatile recycling in subduction zones. The fluxes of sedimentary material and fluids from the subducting slab are responsible for the genesis of arc magmas and the occurrence of volcanism along convergent plate boundaries. The estimates of production rates of major and trace gas components, using instrumentally measured SO_2 fluxes, have shown that the amount of volatiles released from volcanoes are to a large extent balanced by those supplied from various sources, such as the crust, the mantle and subducted material (Andres and Kasgnoc 1998; Hilton et al. 2002; Wallace 2005; Mather et al. 2006; Taran 2009). A

number of workers have used different methods for distinguishing potential contributions to the total volatile input/output—the mantle wedge, arc crust or the sedimentary and basaltic layers of the subducting slab (Varekamp et al. 1992; Sano and Marty 1995; Fischer et al. 1998, 2002, 2008; Sano et al. 1998, 2001; Hilton et al. 2002; Shaw et al. 2003; Wallace 2005; Taran 2009). Fischer et al. (1998) used chemical and isotopic composition of CO_2, N_2 and He in gases of Kudryavy volcano, located at the southern part of the Kurilian arc, to show that for this part of the Kamchatka-Kurile subduction zone, the volatiles discharged from this single volcano could be supplied from the subducted slab and mantle wedge alone, without contribution from the underlying arc crust.

Mutnovsky volcano is another typical subduction-type volcano at the Kamchatka-Kurile subduction zone, located about 1000 km to the north of Kudryavy, with continous high-temperature fumarolic activity and frequent phreatic eruptions. The volcano is characterized by a series of thermal manifestations in its craters including high-temperature (>600°C) fumaroles, ultra-acidic boiling pools, a crater lake, steaming grounds and spectacular 600-m high crater walls of altered rocks covered by a thick glacier (Fig. 1). On its northern slopes several groups of steam vents and thermal springs demonstrate the presence of a powerful geothermal system. Almost all the fumarolic fields of the volcano are easily accessible except high-temperature fumaroles from so-called "Active Funnel", the youngest, 60-m deep, 250-m wide crater with nearly vertical walls and a permanent ~1 km-high gas plume.

Mutnovsky is one of the best studied volcanoes in Kamchatka. Soon after the 1960–61 phreatic eruption, two papers on the gas composition were published (Vakin et al. 1966; Serafimova 1966). Serafimova (1966) presented a detailed map of the Bottom fumarolic field of the main crater showing temperatures and flow rates of fumaroles, and reported 9 chemical analyses of the hottest fumaroles, with two analyses from the Active Funnel. Polyak et al. (1985) and Muraviev et al. (1983) have estimated the heat output from the volcano. Taran et al. (1986, 1987) studied chemistry and isotopic compositions of hydrothermal fluids from natural manifestations and the first geothermal wells of the Mutnovsky geothermal field. Taran et al. (1992) published a study of the Mutnovsky fumarolic system with a conceptual geochemical model of the volcano-hydrothermal activity of the volcano. They presented chemical and isotopic data for one more fumarole from the Active Funnel, with a temperature of 360°C.

Here we report our data on the gas geochemistry obtained as the result of extensive sampling of all fumarolic fields in the volcano craters and main geothermal manifestations and wells of the geothermal field performed during the 2001 and 2006–2007 field seasons. More than 20 samples were taken from fumaroles of Active Funnel. For the first time a comprehensive data set is presented on light hydrocarbons in volcanic and hydrothermal gases of Mutnovsky, as well as the He and Ar concentrations and nitrogen isotopic composition.

One of the main goals of this study is to estimate the sources of volatiles contributing to the Mutnovsky volcanic and hydrothermal fluids using a large set of geochemical data that includes the composition of major (H_2O, CO_2, S, HCl, N_2, H_2) and trace (Ar, He, CO, CH_4, and C_2–C_4 hydrocarbons) species, $^3He/^4He$, D/H, $^{18}O/^{16}O$ and $^{15}N/^{14}N$ isotopic ratios. We attempt to derive the composition of the parent magmatic gas and to estimate the mantle, crust and slab fractions in the magmatic discharge of Mutnovsky.

General setting

Mutnovsky volcano is located ~75 km to the south of the main city of the Kamchatka district Petropavlovsk-Kamchatsky (Fig. 1). It has an elongated edifice composed of merged stratocones (Fig. 2a). The highest point is 2323 m asl (52.35 N, 158.27 E). Two large joined craters, Northern and Southwest, of 1.3×1.3 and 1.5×2 km^2, respectively, are situated ~1 km westward from the main summit. The young active crater with the most intensive emissions, named "Active Funnel" cuts the rim of the large Southwest crater (Fig. 2b).

Mutnovsky is located ~20 km from the Pacific coast, ~200 km from the Kamchatkan trench and belongs to the Eastern (frontal) volcanic belt of Kamchatka (Fig. 1). The depth to the Mohorovicic discontinuity beneath Mutnovsky is 22 km, the depth to the Benioff zone is 90–110 km (Gorbatov et al. 1997). The first detailed geological description of Mutnovsky was reported by Marenina (1956). The volcano resides on a basement that is interpreted as a complex of Paleogene-Neogene volcanogenic-sedimentary rocks with domination of volcanogenic component ranging from basalts to rhyolites (Selyangin 1993). All these rocks are partly metamorphosed to greenschist facies and altered; propylitization is the most common type of the hydrothermal alteration. A large (15×15 km^2) Miocene Akhomten granodiorite intrusion borders Mutnovsky from the east.

The Mutnovsky Geothermal Field extended 6–7 km to the north of the Mutovsky volcano (Fig. 2a). Tens of geothermal wells, 1–2.5 km-deep, produce fluid from 240–300°C geothermal aquifer for operating a 60 MW power-plant.

According to Melekestsev et al. (1987), the last eruption of the volcano that provided juvenile basaltic material, occurred in the 1848. During the 20th century, six small phreatic

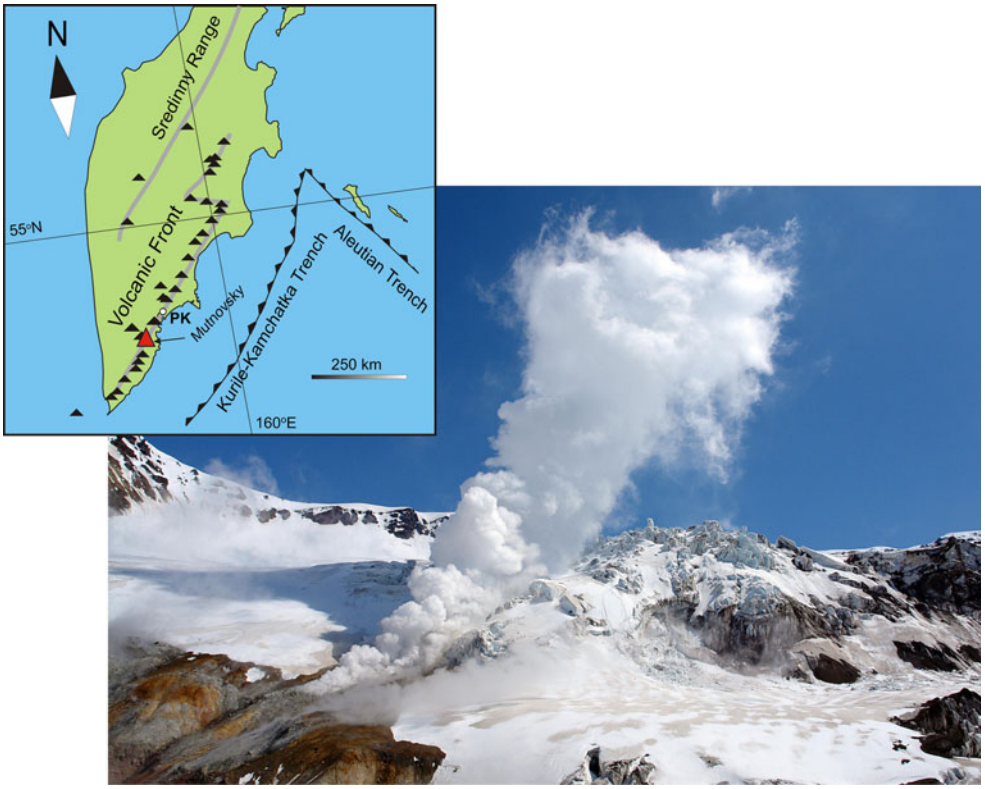

Fig. 1 Upper Field fumaroles in the crater of Mutnovsky volcano. Inset: location of Mutnovsky volcano, southern Kamchatka (*red triangle*). Triangles are Holocene and active volcanoes. *PK* Petropavlovsk-Kamchatsky

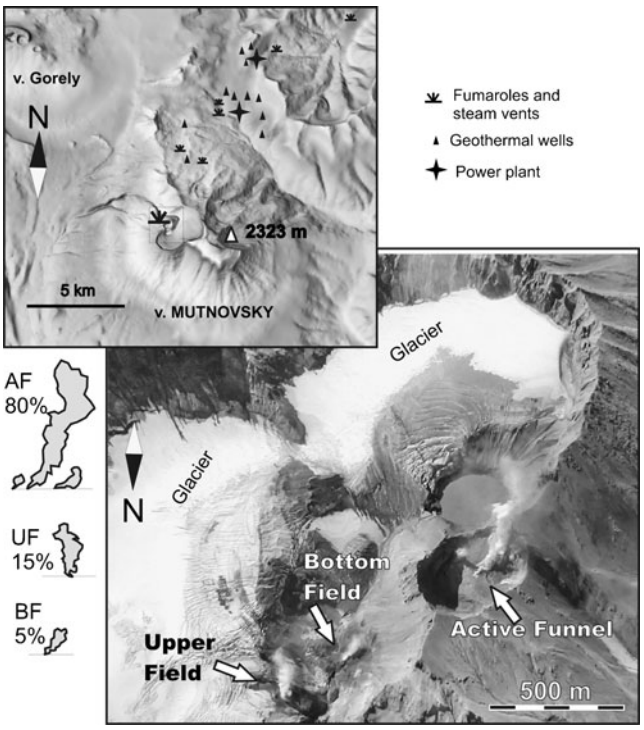

Fig. 2 **a**: Digital map of the Mutnovsky area with volcanic edifices and geothermal field. **b**: Craters of Mutnovsky volcano with fumarolic fields. The visible area of the contours of fumarolic plumes (left side of the down cartoon) may be used for estimation of the relative steam output (see text for explanations). AF, BF and UF are Active Funnel, Bottom Field and Upper Field, respectively

eruptions have been recorded: 1904, 1916–17, 1927–29, 1939–40, 1960–61 and 2000. The 1960–1961 and 2000 eruptions are well documented (Kirsanov 1964; Serafimova 1966; Vakin et al. 1966; Zelenski et al. 2002). The last phreatic explosion occurred on the 17th of April 2007.

Eruptive products of Mutnovsky have evolved from basalts to andesites and dacites; the most felsic rocks of the whole volcano are two rhyodacite flows (Selyangin 1993). Duggen et al. (2007) proposed the dehydration of the slab sediments and altered basalts as the main factor providing the parent magma generation of the Mutnovsky volcano. The slab component beneath Mutnovsky is inferred to be primarily a hydrous fluid with a minor amount of a silicate melt.

Sampling and analysis

Samples of fluids from five sampling sites were taken (Fig. 2). Two of them are located in the Northern Mutnovsky crater: the Bottom Field (BF) and the Upper Field (UF). The third site is Active Funnel (AF) which is the most recent crater of Mutnovsky with oval shape (~250 m in diameter) and steep to vertical walls from 60 to 200 m high. Fumaroles in this young crater are located on the bottom and within the 1/3 lowest part of the southern wall. The hottest vent had 620°C in 2006. Discharge conditions at the Bottom Field are quite various and include

boiling-point and hot fumaroles (up to 280°C), boiling springs, drainless boiling pools with some of them filled with the ultra-acidic brine; mud pools and bubbling gas in the Vulcannaya stream which drains all water discharges of the Northern crater. Upper Field is located on the western slope of the Northern crater, 20–50 m above the crater floor, close to the front of the glacier. There are several powerful "roaring" fumaroles there with temperatures up to 280°C (Fig. 1).

Volcanic and hydrothermal gases were sampled into 100–250 ml Pyrex ampoules with a Teflon stopcock filled with 50 ml of 4 N KOH solution, according to the procedure developed by Giggenbach (1975). At a sampling site, a 20×1000 mm silica tube was inserted into a fumarole vent. An inner 8 mm silica tube connected to short silicone rubber tubing was put into the outer tube to let gas flow freely with a flow rate enough to prevent any condensation. Additionally, 50 ml of gas condensate was collected at each sampling site by pumping gas trough two sequentially connected bubblers cooled by a snow-water mixture. Gas temperature was measured by a thermocouple inserted 10–20 cm inside the vent.

Samples from the geothermal field are represented by steam vents (SV) and geothermal wells (W). Temperature of all steam vents was ~96°C corresponding to the boiling point at elevation of the geothermal field (800–900 m above sea level). Temperature of well fluids can be estimated between 250 and 300°C for the deep water-dominated wells and ~240°C for the shallow wells drilled into the steam cap. All wells are characterized by fluid enthalpies within a range of 900–2700 kJ/kg. Gas samples from geothermal wells were taken from the steam line of cyclone separators attached to each well. Separation pressure was near 8 atm everywhere.

In the laboratory a split of non-absorbed gases from the headspace was transferred into 10 ml ampoules for $\delta^{15}N$ and $^3He/^4He$ isotopic analyses. The headspace gases were analyzed by gas chromatography. Thermal conductivity detector, Ar as a carrier gas, and a packed column with Molecular Sieves 5A were used for determination of H_2 and He. Separation of Ar from O_2 was performed using a CT-III (Altech) packed column and He as a carrier gas. Same column was used for the analysis of N_2, O_2, CO, and CH_4. Flame ionization detector and a packed column with Al_2O_3 were used for the analysis of light hydrocarbons C_2–C_4 and CH_4 in low concentrations. Low concentrations of CO in low-temperature gases were determined using a packed MS 5A column coupled with a high-sensitivity Reduced Gas Detector (detection limit ~10^{-4}%). Detection limits for N_2, O_2 and Ar were 0.01, 0.01 and 0.005 vol%, respectively. For H_2 and He detection limit was estimated to be better than 0.001 vol%. Sensibility for methane was ~0.05 vol% with the thermal conductivity detector and better then 10^{-5} vol% for the flame ionization detector. Sulfate (total sulfur after oxidation of the alkaline condensate by H_2O_2), chloride and fluoride were measured in the oxidized alkaline solution by ion chromatography. The CO_2 concentration was obtained by volumetric method after adding to an aliquot of the oxidized alkaline condensate an excess of concentrated H_2SO_4 and measuring the volume of the liberated CO_2.Concentrations of SO_4^{2-} in selected samples were verified by the gravimetric determination of precipitated $BaSO_4$. Uncertainties for the gas and chemical analyses were within 5%.

Condensates were analyzed for $\delta^{18}O$ and δD in the Institute of Ore Deposits (Moscow) and Instituto de Geofisica, UNAM, Mexico. The mass-spectrometric measurements in both laboratories were carried out by the DELTA Plus mass-spectrometer (Finnigan) coupled with the H/D device. Accuracy for $\delta^{18}O$ was about 0.2 ‰, for δD—about 0.5‰.

Helium and nitrogen isotopes were analysed in the Institute of Geophysics and Volcanology (INGV), Palermo. The $^3He/^4He$ ratios were measured by a static vacuum mass spectrometer (VG-5400TFT, VG Isotopes) modified to detect $^3He/^4He$ ion beams simultaneously, reducing the error of the $^3He/^4He$ measurements in ^3He-rich gases down to values lower than 0.1%. $^3He/^4He$ ratios were corrected for the atmospheric contamination on the basis of the difference between the $^4He/^{20}Ne$ of the sample and in the air (Sano and Wakita 1985). $\delta^{15}N$ measurements were carried out on a Finnigan Delta Plus XP continuous-flow IRMS coupled with a TRACE GC equipped with a MS 5A PLOT capillary column (60 m, ID 0.32 mm). The amount of ^{36}Ar, the isotopic composition and amount of nitrogen, have been analyzed directly and simultaneously on the same aliquot of a sample with a single injection (Inguaggiato et al. 2006). This procedure allows the correction of the air contamination and the normalization of the results. The analytical precision of $\delta^{15}N$ measurements is better than 0.15‰ (1σ) as determined on ten air samples.

Results and discussion

Gas output rates

On September the 1st 1999 Fischer (unpublished) has measured SO_2 flux of Mutnovsky with COSPEC. The flux was estimated to be 200±50 tons/day. Assuming the weight-average SO_2 content in AF gases at 2.0% (Taran et al. 1992; this work) the total discharge will be of 10000± 2500 t/d or 115±29 kg/s of volcanic vapor from the Active Funnel.

To estimate outputs from other fumarolic fields we used a comparative empirical method described by Hochstein

and Bromley (2001). The heat transferred to the atmosphere by fumarolic plumes is proportional to the visible plume area registered at the same time. Comparing areas of the reference combined plume of AF and fumarolic plumes of BF and UF fields, the next by magnitude output was accounted to the Upper Field at 20±5 kg/s and only 6.6± 1.5 kg/s is emitted from the Bottom Field (Fig. 2b). The absolute values are 3–5 times lower than those from Vakin et al. (1976) and Polyak et al. (1985). However, we believe that the relative output from fumarolic fields (~0.8 : 0.15 : 0.05) is estimated by this method with the acceptable accuracy.

Variations in chemical composition of volcanic and hydrothermal gases

Chemical and isotopic compositions of gases are listed in Tables 1, 2 and 3. Concentrations of N_2 and Ar are corrected on the direct air contamination using the measured O_2 content: $N_{2,c} = N_{2,m} – 3.72 \times O_2$ and $Ar_c = Ar_m – O_2/22.43$, where subscripts c and m stand for "corrected" and "measured", respectively. Such a correction does not take into account O_2 consumed by the oxidation of sulfur species and hydrogen. AF fumaroles have the highest CO_2-S- N_2-He-Ar absolute concentrations and the lowest H_2O. Gases from the Bottom Field have a higher water content compared to the Active Funnel. The UF gases show an interesting combination of a relatively high gas temperature up to 280°C together with a very high concentration of water vapor, low concentrations of other components (1–2%) and a high absolute concentration of methane. Relative concentrations of N_2, Ar and CH_4, are shown in Fig. 3a. Important sources for these components are thought to be air-saturated water (ASW) and hydrothermal water-rock interaction (Giggenbach 1992a; Taran and Giggenbach 2003). All gas compositions are plotted here including gases from geothermal wells and hydrothermal steam vents. Very low relative CH_4 content and N_2/Ar ratios much higher than air-ASW values are characteristic for all AF fumaroles, independently of the temperature. Hydrothermal gases show a mixing between CH_4-poor and CH_4-enriched components both associated with a meteoric-hydrothermal source. The highest relative (and absolute) concentration of methane is observed in the Upper Field gases. These gases are also characterized by elevated, non-atmospheric, N_2/Ar ratios and their compositions apparently lie on a trend between a high N_2/Ar, low CH_4 magmatic component and defined above a CH_4-enriched meteoric-hydrothermal component. Another ternary plot for the "acidic" components CO_2-S-Cl derived mostly from the degassing magma is shown in Fig. 3b for gases from the crater. It follows from this diagram that the AF gases have relatively constant HCl concentrations and variable CO_2 and S with a negative correlation between them. The BF gases have the highest relative HCl concentration, and the UF gases are characterized by the lowest relative S and HCl.

The Giggenbach N_2-Ar-He diagram (Giggenbach 1992a) shown in Fig. 3c for all gases, hydrothermal and volcanic, discriminates hydrothermal gases with a low He relative content and atmospheric N_2/Ar ratios, and high N_2/Ar volcanic gases with non-atmospheric (magmatic?) nitrogen. Gases from the Active Funnel with the highest N_2/Ar ratio (and hence, the highest fraction of the non-atmospheric nitrogen) are characterized by a high N_2/He ratio of 2000–3000.

Isotopic composition and origin of water

The isotopic data for rain and snowmelt water at the Mutnovsky area range in $\delta^{18}O$ from −19.1‰ to −10.7‰ and in δD from −124‰ to −72.6‰ (Taran et al. 1987; Cheshko and Esikov 1990). On the Craig plot, δD vs $\delta^{18}O$, (Fig. 4a) the meteoric water compositions are shown as a linear trend that represents the local meteoric water line (LMWL) for Kamchatka (Cheshko and Esikov 1990). This trend can be fitted with an expression $\delta D = (8 \pm 0.2) \cdot \delta^{18}O + 16.5 \pm 1.5$. Thus, the local meteoric water line is shifted approximately 6‰ above the global meteoric water line ($\delta D = 8\delta^{18}O + 10$, Craig 1961).

Only one point of the meteoric water composition is shown in Fig. 6 with δD=−112‰ and $\delta^{18}O$=−15.7‰ that corresponds to water from the crater lake formed after the 2000 phreatic eruption (Fig. 2) in the Southwest crater of Mutnovsky. The lake was filled by water from melting of perennial snow and ice accumulated inside the crater for many years (Zelenski et al. 2002). As the sample was taken soon after the lake had appeared, evaporation could not affect significantly its isotopic composition. Therefore this sample can be referred as the "average meteoric water" for the crater of the Mutnovsky volcano.

Hydrothermal vapors (geothermal wells and steam vents) have water isotopic composition close to meteoric water values. Water vapor from steam vents and geothermall wells (separators) both have a negative $\delta^{18}O$ shift of ~1‰ from the LMWL. As it has been shown by Taran et al. (1987), this negative O-shift associates with the steam separation at temperatures close to 200°C. At these temperatures the fractionation of hydrogen is close to zero but vapor is depleted in ^{18}O (Horita and Wesolowski 1994). In contrast, water from geothermal wells is ~1−1.5‰ enriched in ^{18}O. This O-shift due to water-rock interaction is smaller than for many other high-temperature hydrothermal systems indicating a high water-rock ratio in the Mutnovsky aquifer which is in turn in agreement with a very diluted character of the deep hydrothermal water (~200 ppm of Cl, Taran et al. 1986, 1987).

Table 1 Chemical composition (mmol/mol in the total discharge) and water isotopes (per mil vs. V-SMOW) of volcanic and hydrothermal gases from fumaroles in the crater of Mutnovsky volcano and steam vents and geothermal wells of Mutnovsky geothermal field. bd – below detection limit; empty cell - not determined. N_2 and Ar are corrected on the air contamination (see text). All geothermal wells were sampled several times during 2006. The data for wells are mean values over 4-5 analyses

NN°	Date	t°C	$\delta^{18}O$	δD	S	HF	HCl	CO_2	H_2O	NH_3	He	H_2	CO	Ar_c	N_{2c}	CH_4	N2/He	N_2/Ar
Active funnel																		
1	09.2001	507	−3.5		11.49		2.03	14.08	973.0		7.98E−05	0.309	0.002431	0.00022	0.199	0.000108	2494	905
2	09.2001	196	−3.2		12.00		0.92	9.23	977.9		5.74E−05	0.002	0.000005		0.098	0.000119	1708	
3	09.2001	309	−4.6		7.01		1.80	14.21	977.9		9.26E−05	0.008	0.000007	0.00103	0.313	0.000107	3382	304
4	09.2001	240	−0.9		17.62		2.38	11.22	969.9		6.76E−05	0.008	0.000005	0.000126	0.139	5.36E−05	2056	1103
5	09.2001	410	−2.3		12.35		2.85	14.86	971.6		8.58E−05	0.050	0.000127	0.00016	0.174	7.6E−05	2028	1088
6	09.2001	450	1.0		18.39		2.54	10.76	969.4		6.66E−05	0.131	0.000229	0.00089	0.157	4.8E−05	2357	176
7	09.2001	383	−4.1		10.76		1.70	16.69	971.6		0.000107	0.034	5.97E−05	0.00109	0.379	0.000152	3533	348
8	09.2007	425	−2.1	−49.5	1.03	0.87	0.07	5.68	993.1		0.000139	0.125	0.00060	0.00030	0.349	0.00015	2518	1160
9	09.2007	380	−0.7	−58.4	22.83	0.34	1.81	6.09	968.7		6.65E−05	0.036	0.00002	0.00025	0.141	0.00002	2122	566
10	09.2007	543	−1.4	−53.5	12.07	0.31	2.35	23.72	960.3	0.033	0.000152	0.716	0.01228	0.00041	0.467	0.00048	3080	1138
11	09.2007	594	−1.1	−54.5	13.16	0.36	2.38	26.04	956.8	0.010	0.000162	0.779	0.01042	0.00040	0.443	0.00034	2737	1116
12	09.2007	590	0.5	−45.3	12.69	1.07	2.33	24.65	958.2		0.00016	0.664	0.00632	0.00019	0.369	0.00022	2304	1967
13	09.2007	580	−1	−46.5	14.08	0.74	2.46	19.72	967.1	0.030		0.527	0.00378	0.00025	0.346	0.00007		1393
14	09.2007	315	−0.65	−55.2	20.21	0.22	2.02	11.26	966.1		8.69E−05	0.011	0.00002	0.00018	0.175	0.00005	2017	952
15	09.2007	543	1.3	−42.7	17.58	1.00	2.72	16.06	965.9		0.00012	0.315	0.00144	0.00032	0.224	0.00007	1877	701
16	09.2007	357	−2.5	−58.9	14.07	0.31	2.10	12.64	970.6		8.17E−05	0.030	6.26E−05	0.00019	0.224	0.00015	2748	1167
17	09.2007	400	−4.2	−72.6	8.12	0.24	1.32	23.61	966.3		0.000144	0.056	7.26E−05	0.00118	0.332	0.00068	2300	281
18	09.2007	205	−4.3	−79	15.25	0.09	0.78	2.78	981.0		4.96E−05	0.006	bd	0.00013	0.070	0.00049	1415	537
19	09.2007	543	1.5	−41.1	17.58	1.00	2.80	16.56	965.9	0.005	0.00012	0.315	0.001438	0.00032	0.224	0.00007	1877	701
20	09.2007	280	−0.4	−57.4	24.47	0.26	1.68	1.83	971.7		2.82E−05	0.006	bd	0.00011	0.029	0.00021	1029	263
21	09.2007	380	−5.9	−73.4	10.28	0.31	2.27	21.14	965.6	0.017	0.000133	0.039	3.75E−05	0.00014	0.341	0.00086	2554	2458
Bottom Field																		
22	09.2001	153	−5.9	nd	3.62	nd	2.21	5.12	988.5		8.7E−05	0.0085	7.53E−05	0.0008	0.14	0.002885	1610	175
23	09.2007	111	−8.84	−97.6	2.94	0.01	0.45	2.85	993.7		9.32E−06	0.003	4.66E−06	0.00013	0.044	0.00279	4773	347
24	09.2007	137	−5.17	−82.2	3.79		1.22	3.05	991.9	0.023	2.27E−05	0.002	1.41E−06	0.00018	0.064	0.00106	2802	351
25	09.2007	263	−4.68	−86.4	3.67	0.07	1.92	2.58	991.7	0.011	2.6E−05	0.009	6.84E−07	0.00004	0.045	0.00297	1742	1038
26	10.2006	120	−4.94	−77.4	6.73	0.01	2.63	5.71	984.8		5.23E−05	0.005	bd	0.00011	0.078	0.00307	1492	693
27	10.2006	98	−6.79	−86.7	2.12		0.03	5.25	992.5		4.89E−05	0.004	1.44E−06	0.00014	0.083	0.00317	1694	596
28	10.2006	186	−5.03	−76.3	2.91	0.01	1.17	1.72	994.1	0.011	4.82E−05	0.006	1.28E−06	0.00014	0.070	0.00332	1452	498
29	10.2006	98	−5.43	−82.1	1.61		0.03	3.11	995.2		4.58E−05	0.005	2.21E−06	0.00014	0.069	0.00261	1512	485
30	10.2006	105	−5.16	−76.6	3.26		0.91	2.10	993.6		5.18E−05	0.002	1.32E−06	0.00012	0.080	0.00187	1544	643
31	09.2007	125						5.33	994.6		7.56E−06	0.003	bd	0.00013	0.036	0.00127	4806	272
32	09.2007	218						3.38	996.6		1.38E−05	0.002	1.15E−06	0.00007	0.029	0.00120	2086	411
33	10.2007	190						4.53	995.4		3.1E−05	0.005	2.32E−06	0.00024	0.073	0.00280	2369	303
34	10.2007	150						4.75	994.9		0.000122	0.002	bd	0.00333	0.325	0.00205	2653	98
35	10.2007	115						3.73	996.2		3.87E−05	0.003	1.07E−06	0.00030	0.074	0.00184	1901	246
36	10.2007	135						0.10	999.9		4.37E−05	0.001	1.21E−06	0.00029	0.079	0.00272	1796	274

37	10.2007	150					3.95	995.8		4.49E−05	0.002	5.93E−05	0.00201	0.220	0.00231	4909	110
Upper field																	
38	2001	281	−11.3		1.03	0.07	5.68	993.1		1.12E−05	0.004996	6.34E−06		0.091	0.03225	8159	
39	09.2007	96	−13.7	−116	0.73	0.02	2.91	995.1			0.002	bd	0.01442	1.175	0.02407		188
40	09.2007	138	−9.5	−102.8	0.72	0.13	5.85	993.2		6.39E−06	0.001	bd	0.00018	0.034	0.01474	5346	276
41	09.2007	98	−11.2	−107.4	0.49	0.22	1.63	997.6	0.016	7.04E−06	0.001	bd	0.00018	0.050	0.01980	7057	188
42	09.2007	186	−11.4	−103.5	0.85	0.01	2.40	996.7		8.28E−06	0.001	bd	0.00024	0.046	0.01978	5520	248
43	10.2006	149	−11.0	−106.9	0.81	0.06	1.65	997.4		1.42E−05	0.004	8.4E−07	0.00013	0.033	0.02205	2295	274
44	10.2006	212	−11.6	−104.1	0.88	0.07	5.01	994.0	0.032	2.03E−05	0.003	8.88E−07	0.00014	0.039	0.02395	1915	199
45	10.2006	285	−11.6	−104.8	0.80	0.09	1.66	997.4	0.063	9.68E−06	0.007	9.49E−07	0.00019	0.038	0.02281	3901	270
46	10.2006	148	−11.7	−106.6	0.88	0.12	2.33	996.6		1.12E−05	0.001	bd	0.00014	0.037	0.02503	3256	244
47	10.2006	231	−11.7	−107.8	0.83	0.08	2.08	996.9		1.35E−05	0.005	9.75E−07	0.00015	0.036	0.02739	2697	203
48	10.2006	248	−11.2	−106.5	0.80	0.08	3.88	995.2	0.059	1E−05	0.007	9.31E−07	0.00019	0.039	0.02028	3904	258
49	10.2006	172	−11.9	−107	0.77	0.07	2.40	996.7		1.21E−05	0.005	8.72E−07	0.00013	0.035	0.02239	2885	
Steam vents																	49
50	05.2007	96						999.6			0.179	1.02E−05	0.00119	0.058	0.01730		60
51	05.2007	96	−16.6	−108.2	0.93	0.01	0.29	999.1		7.15E−06	0.444	bd	0.00163	0.098	0.01562	13719	56
52	05.2007	96	−15.5	−106.8	0.44	0.00	1.77	998.0		9.82E−06	0.140	3.5E−05	0.00120	0.067	0.00346	6871	52
53	05.2007	96				0.00		999.6			0.258	7.51E−06	0.00182	0.095	0.01094		69
54	05.2007	96	−14.5	−102.4	0.10	0.02	0.89	999.0		1.93E−06	0.043	bd	0.00021	0.015	0.00387	7515	68
55	05.2007	96				0.00	1.76	998.0			0.164	bd	0.00035	0.024	0.01392		
56	05.2007	96				0.01	0.69	998.4									
57	05.2007	96				0.00	2.71	996.8									
58	05.2007	96				0.05	0.05	999.9									
	# well	H kJ/kg	Geothermal wells														
59	24	910	−14.0	−109.2	0.06		0.22	999.70		6.50E−07	0.001	2.50E−07	0.00006	0.0030	0.00096	10769	49
60	048	1105	−13.5	−104.9	0.06		0.32	999.60		8.79E−07	0.001	5.17E−07	0.00012	0.0106	0.00026	12059	86
61	049	1018	−13.2	−103.7	0.08		0.88	998.98		1.79E−06	0.005	3.77E−06	0.00056	0.0394	0.00145	21970	70
62	013	1425	−13.4	−104.6	0.14		0.57	999.24		1.15E−06	0.023	6.01E−06	0.00015	0.0150	0.00168	13034	99
63	26	2650	−14.2	−103.0	0.11		1.00	998.80		4.15E−06	0.027	bd	0.00090	0.0403	0.00182	9699	45
64	A-2	1293			0.12		0.38	999.48		2.85E−07	0.006	7.68E−07	0.00004	0.0024	0.00037	8361	54
65	029W	1297	−13.2	−110.0	0.11		0.45	999.41		2.85E−07	0.015	bd	0.00005	0.0023	0.00044	7924	42
66	GK-1	1166	−14.1	−107.4	0.12		0.43	999.52		3.85E−07	0.027	1.93E−06	0.00009	0.0045	0.00126	11675	50
67	016	2640			0.21		0.97	998.76		1.18E−06	0.045	1.69E−06	0.00021	0.0109	0.00188	9277	52
68	037	1519	−13.2	−103.0	0.08		0.65	999.23		1.18E−06	0.006	2.36E−06	0.00013	0.0055	0.00327	4691	43
69	042	1113			0.08		0.41	999.46		1.12E−06	0.001	1.66E−06	0.00042	0.0210	0.00100	18729	50
70	4E	1153			0.06		0.36	999.54		8.79E−07	0.001	1.4E−06	0.00027	0.0163	0.00072	18534	60
71	053	1108			0.07		0.25	999.62		3.81E−06	0.002	bd	0.00048	0.0327	0.00070	8584	68

Table 2 Isotopic compositions of He (R/R_a, where R is $^3He/^4He$ in a sample and Ra= 1.4×10^{-6}—isotopic composition of He in air) and N_2 ($\delta^{15}N$ relative air) in volcanic and hydrothermal gases of Mutnovsky. Helium ratios are corrected on air contamination using $^4He/^{20}Ne$. Excess N_2 is calculated from $N_2/^{36}Ar$ as $(1-r_a/r)\times 100\%$, where r and r_a are $N_2/^{36}Ar$ in a sample and in air (asw), respectively. NH_3/N_2 ratios are done as mean values for each group of samples

Date	R/Ra	He/Ne	$\delta^{15}N$	$N_2/^{36}Ar$	N_2,ex % (asw/air)	T°C	NH_3/N_2
		Active funnel					
09/2007	5.29	38	3.3	186420	94/87	543	
09/2007	5.52	67	1.6	58081	81/58	594	
09/2007	6.58	28	1.9	63250	82/61	315	
09/2007	5.57	35	2.5	123077	91/80	543	<0.05>
09/2007	5.99	79	2.8	174652	94/86	400	
10/2007	6.58	13	1.4	39941	72/38	315	
09/2007	5.83	4.3	0.24	29241	62/16	590	
		Bottom field					
10/2007	7.59	71				137	
10/2007	7.67	126	0.16	77710	86/68	263	<0.3>
10/2003	7.36	6.1				96	
		Upper field					
05/2006	6.98	31	0.57	52580	77/53	285	
05/2006	6.59	36	−1.0	26578	59/7.2	248	<1.0>
		Steam vents					
23/10/07	6.06	4.9	−0.08	14710	24/−68	96	
23/10/07	6.66	5.1	−0.15	18592	40/−33	96	<1.0>
23/10/07	5.47	4.3	0.23	16728	33/−47	96	
		Geothermal wells				N°well	
23/10/07	3.51	25	−1.80	16674	33/−47	024	
23/10/07	3.97	14	0.30	17819	37/−38	049	<0.8>
23/10/07	5.89	15	−0.33	19517	43/−26	A2	
23/10/07	3.99	3.0	0.13	20651	46/−19	013	
23/11/07	5.77	3.0	−3.4	15452	27/−60	045	
		Bubbling gas					
23/11/07	5.97	2.1				45	
23/11/07	6.53	5.0				60	
23/11/07	5.13	1.2				47	
air	1.0	0.29	0.0	24660			
asw	1.0	0.25	0.0	11210			

Isotopic composition of volcanic vapors from crater fumaroles (Fig. 4a) is typical for the subduction type volcanoes (Sakai and Matsubaya 1977; Taran et al. 1989; Giggenbach 1992b). Most of the δD-$\delta^{18}O$ data points lay close to the mixing trend between slightly positively O-shifted meteoric waters and "andesitic" waters (Taran et al. 1989). "Andesitic" (Taran et al. 1989) or "arc-magmatic" (Giggenbach 1992b) water is thought to be the subducted and partially altered seawater releasing through arc volcanoes. The δD-HCl relationship shown in Fig. 4b is also similar to that observed for other arc volcanoes with high-temperature, "magmatic", fumaroles (Taran et al. 1995) indicating a common source of Cl and water enriched in D.

The Upper Field fumaroles heated up to 280°C discharge almost pure meteoric steam with a very low chloride and a narrow range of isotopic composition: δD=−106±2‰, $\delta^{18}O$=−11.5±0.5‰. The steam is slightly ^{18}O-shifted (Fig. 4a). A shallow mixing with the ice melt water from glacier for this, closest to the glacier, fumarolic field, seems to be negligible. A significant scattering of the Bottom Field points may indicate some more complicated processes of steam-brine separation beneath the crater floor as mentioned by Taran et al. (1992).

According to Bindeman et al. (2004), a value of +5.9± 0.5‰ can be accepted for $\delta^{18}O$ of lavas of Mutnovsky. Extrapolation of the mixing line to this value gives for δD of the parent magmatic fluid of Mutnovsky a value of −19‰.

Fractions of magmatic fluid for most important fumarole groups can be calculated according to their relative positions on the mixing trend (Figs. 4a and 12b). Gas from the most powerful group of fumaroles in the Active Funnel, which is responsible for at least 80% of the total emission of the volcano, contains 61±3% of magmatic fraction. At the same time, the second by magnitude Upper Field (~15% of the total emission) discharge gas with not more than 2% of magmatic fluid.

Table 3 Light hydrocarbons in volcanic and hydrothermal fluids of Mutnovsky. Concentrations are normalized to methane ($c_i = C_i/C_{CH4}$). For absolute concentrations of methane see Table 1

NN°	CH_4	C_2H_6	C_2H_4	C_3H_8	C_3H_6	C_4H_{10}	T°C
				Active	funnel		
8	1	0.0024	0.0054	2.8E−04	0.0065	1.9E−04	425
9	1	0.0022	6.1E−04	5.1E−04	2.4E−04	2.3E−04	543
10	1	0.0024	0.0044	0.0022	0.0016	7.0E−04	543
11	1	0.0026	7.1E−04	1.3E−04	0.0019	bd	594
12	1	0.0023	0.0032	7.9E−04	0.0016	5.0E−04	590
13	1	0.0020	0.0036	4.0E−04	0.0022	2.9E−04	580
14	1	0.0025	8.9E−04	3.8E−04	9.0E−04	2.9E−04	315
15	1	0.0027	0.0062	6.9E−04	0.0038	4.3E−04	543
16	1	0.0022	0.0011	3.0E−04	8.7E−04	1.2E−04	357
17	1	bd	1.1E−04	2.3E−05	1.4E−04	2.5E−05	400
18	1	0.0025	2.8E−04	1.4E−04	7.1E−05	1.0E−04	205
19	1	0.0027	0.0062	6.9E−04	0.0038	4.3E−04	543
20	1	0.0044	0.0012	5.0E−04	0.0011	1.4E−04	280
21	1	0.0020	3.5E−04	1.7E−04	1.9E−04	4.0E−05	380
				Bottom	field		
22	1	0.0013	4.2E−05	3.0E−05	1.4E−05	2.3E−05	111
23	1	0.011	7.8E−05	1.3E−05	9.8E−05	1.1E−05	137
24	1	0.017	0.012	1.0E−05	7.6E−06	7.3E−06	263
25	1	0.015	bd	3.3E−06	6.7E−06	6.2E−06	98
26	1	0.026	bd	1.1E−04	2.4E−05	2.6E−05	186
27	1	0.016	bd	6.2E−06	2.2E−05	6.7E−06	98
28	1	0.015	bd	1.6E−05	2.9E−05	4.4E−04	105
29	1	0.026	4.5E−05	4.3E−05	1.2E−05	1.4E−04	125
30	1	0.017	7.2E−04	8.5E−06	1.1E−06	6.5E−04	218
31	1	0.025	8.2E−05	2.0E−05	9.1E−06	2.2E−04	190
32	1	0.011	0.0038	6.8E−05	6.7E−05	2.4E−04	150
33	1	0.019	2.0E−04	4.9E−05	9.0E−06	2.5E−04	115
34	1	0.016	1.3E−04	1.5E−05	2.9E−06	3.5E−06	135
35	1	0.0092	9.0E−05	1.5E−05	1.3E−05	1.1E−05	150
				Upper	field		
38	1	0.0063	bd	2.3E−04	3.9E−06	5.6E−06	96
39	1	0.0087	bd	2.5E−04	4.2E−06	3.3E−06	138
40	1	0.0085	bd	3.7E−04	3.5E−06	2.8E−06	98
41	1	0.0078	bd	3.7E−04	4.9E−06	1.6E−06	186
42	1	0.011	bd	2.9E−04	6.9E−07	1.6E−06	149
43	1	0.011	bd	3.4E−04	5.7E−06	3.4E−06	212
44	1	0.014	0.0093	3.3E−04	6.0E−06	3.2E−06	285
45	1	0.011	bd	3.0E−04	7.6E−07	1.5E−06	148
46	1	0.011	0.0096	3.3E−04	6.5E−06	1.9E−06	231
47	1	0.013	0.0053	3.6E−04	5.8E−06	3.0E−06	248
48	1	0.015	bd	3.2E−04	6.7E−06	4.7E−06	172
				Steam	vents		
50	1	0.013	4.0E−04	7.1E−04	1.8E−05	6.9E−05	96
51	1	0.020	1.6E−04	4.0E−04	4.4E−05	8.6E−05	96
52	1	0.030	5.1E−05	1.9E−03	7.8E−05	2.1E−04	96
53	1	0.028	5.5E−05	1.7E−03	5.2E−05	1.9E−04	96
54	1	0.0046	9.3E−05	5.7E−04	3.9E−05	9.6E−05	96

Table 3 (continued)

NN°	CH_4	C_2H_6	C_2H_4	C_3H_8	C_3H_6	C_4H_{10}	T°C
55	1	0.035	7.1E−05	4.0E−03	3.0E−05	2.2E−04	96
				Geothermal	wells		
59	1	0.0021	1.5E−04	6.2E−05	1.3E−05	3.4E−05	
60	1	0.024	4.6E−04	0.016	5.3E−04	6.6E−04	
61	1	0.026	3.2E−04	0.0018	6.8E−04	2.6E−04	
62	1	0.0075	0.0014	8.8E−04	1.5E−05	2.6E−05	
63	1	0.024	1.3E−04	0.0019	1.9E−04	4.8E−04	
64	1	0.014	3.3E−04	0.0012	8.9E−05	2.7E−04	
65	1	0.021	1.4E−04	0.0019	2.9E−04	6.3E−04	
66	1	0.019	2.2E−04	0.0011	6.9E−05	2.2E−04	
67	1	0.014	5.9E−05	6.4E−04	2.1E−06	2.2E−05	
68	1	0.021	5,1E−04	0.0019	2.6E−04	8.8E−04	

nd not determined; *bd* below detection limit. Numbers of samples according to Table 1

Major and minor reactive species and chemical equilibria

Hydrogen and carbon monoxide

Many of the chemical and isotopic features observed in volcanic gases can be explained in terms of the attainment of chemical equilibrium among the components of the gas phase itself or within the heterogeneous system involving the gas-rock interaction. Giggenbach (1987) developed a method of geothermometers and geobarometers for volcanic gases using a set of redox-equilibria with $R_H = \log(x_{H2}/x_{H2O})$ as the main variable. According to Giggenbach (1987), the redox-state of high-temperature volcanic gases is controlled by fast reactions between oxidized and reduced sulfur species in the gas phase itself. With decreasing temperature the analytical R_H preserve high values due to quenching of high-temperature values or attaining equilibrium with the rock matrix. The R_H vs temperature diagram for Mutnovsky gases (Fig. 5a) demonstrates a good correspondence of the measured gas compositions in the Active Funnel to the "gas-buffer" control for gases with temperature >300°C and a systematic deviation to more "hydrothermal" values as temperature decreases. Another system which was found to adjust rapidly to conditions into the gas phase itself is $CO\text{-}CO_2$ (Giggenbach 1987; Taran et al. 1995; Chiodini and Marini 1998). Comparison of analytical and theoretical CO/CO_2 ratios, as shown in Fig. 5b, reveals the same behavior as for R_H: at temperatures >300°C the relative concentration of CO is governed by the gas ($H_2S\text{-}SO_2$) buffer and at lower temperature the deviation of data points from the gas buffer line can be related either to quenching of the high-temperature values or to re-equilibration with rock ($FeO_{1.5}$-FeO, or GT-buffer—from Geothermal Buffer) as defined by Giggenbach (1987).

Points for geothermal steam vents lay close to the GT-vapor buffer line, whereas all points for geothermal wells fall into the two-phase region, between GT-liquid and GT-vapor lines.

Methane

Methane in volcanic and hydrothermal gases of Mutnovsky is not in equilibrium within the C-H-O system, similar to observed for many volcano-hydrothermal systems (Taran 1986; Taran and Giggenbach 2003). Three plots "$\log(CH_4/CO_2)$ vs R_H" with the same set of data points and different theoretical equilibrium lines are shown in Fig. 6. Line GT corresponds to the $FeO\text{-}FeO_{1.5}$ rock buffer. The closest to an equilibrium line data points correspond to samples from the highest-temperature (~600°C) AF fumaroles. It could be suggested that CH_4 was equilibrated in the fluid under ~1 kbar pressure. Taran and Giggenbach (2003) have discussed in details processes potentially responsible for the equilibration of hydrocarbons in volcanic and hydrothermal fluids. Since methane and other hydrocarbons in volcanic and hydrothermal systems have predominantly sedimentary origin, the main process leading to the equilibration should be oxidation of methane (decreasing concentrations with increasing temperature) but not reduction of CO_2 because this process even under appropriate reduced conditions is extremely slow kinetically (Giggenbach 1997a; Taran and Giggenbach 2003). Therefore, the oxidation (oxidative hydrolysis or cracking) of hydrothermal methane admixed to the high-temperature AF gases may be responsible for much lower CH_4 concentrations in AF gases.

Hydrocarbons

The histogram in Fig. 7 characterizes the hydrocarbon fraction of volcanic and hydrothermal gases in terms of

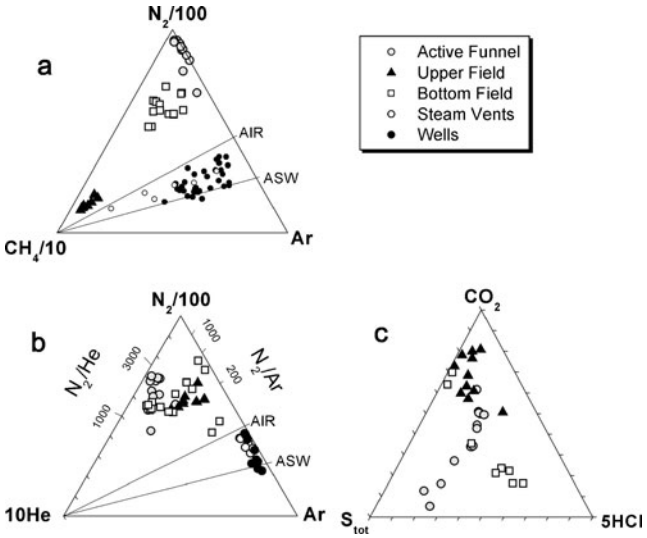

Fig. 3 Ternary diagrams for Mutnovsky volcanic and hydrothermal gases: **a**: N_2- CH_4-Ar; **b**: N_2-Ar-He, and **c**: S_{tot}-CO_2-HCl (mmol/mol basis). See text for discussion

their CH_4/C2+ ratios where C2+ is the sum of concentrations of all C2 to C4 hydrocarbons. The mean value of the CH_4/C2+ ratio of ~60 for all but the Active Funnel hydrocarbons indicates essentially thermogenic origin of hydrocarbons, typical for high-temperature hydrothermal systems and volcanic gases (Welhan 1988; Taran and Giggenbach 2003). Taran et al. (1987, 1992) reported isotopic composition of CH_4 in volcanic and hydrothermal gases of Mutnovsky in the range of −25‰ to −27‰ , typical for thermogenic methane.

Much higher CH_4/C2+ ratios in the AF hot gases most probably is the result of high-temperature hydrolytic oxidation of C2+ hydrocarbons, which is more effective for long hydrocarbon chains than for methane (Arutyunov and Krylov 1998). The only chemical processes that can lead to equilibrium relationships between C2+ hydrocarbons are those without breaking or forming the C-C bonds. The most probable are hydrogenation-dehydrogenation of an alkane-alkene pair like $C_2H_4 + H_2 = C_2H_6$. Taran and Giggenbach (2004) showed that in volcanic gases of White Island the metastable equilibrium is attained between C_2H_6 and C_2H_4 as well as between C_3H_8 and C_3H_6. Gases of Mutnovsky volcano and hydrothermal system show that metastable equilibrium between alkanes and alkenes is attained at temperatures close to the discharge temperatures. Data points in Fig. 8 fall between the equilibrium line at 1 bar (surface) pressure and the line corresponding to equilibrium under pressure of saturated vapor from a hypothetical "brine" as it has been suggested by Giggenbach (1987) for quantifying the temperature-pressure relationship beneath the White Island crater.

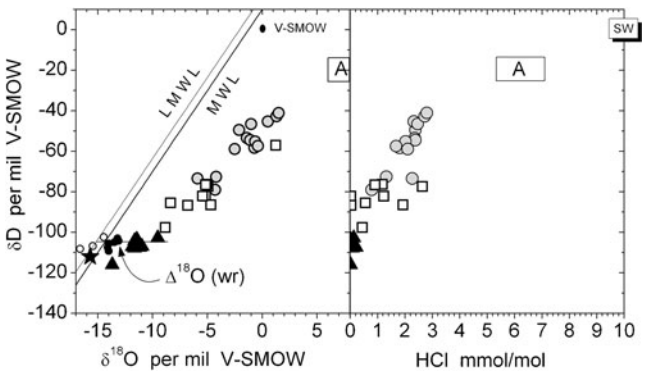

Fig. 4 δD vs δ^{18}O plot for volcanic and hydrothermal vapors of Mutnovsky. For symbols see Fig. 3. LMWL—local meteoric water line—is plotted using data by Cheshko and Esikov (1990) MWL—world meteoric water line, $8\delta^{18}O + 10$ (Craig, 1961). Areas A corresponds to "Arc" or "Andesitic" waters as defined by Taran et al. (1989) and Giggenbach (1992b). SW—seawater. Δ^{18}O (wr) denotes the oxygen isotopic shift due to water-rock interaction (see text)

He as an indicator of the parent magmatic gas composition

Balance calculations concerning the subducted and the releasing through volcanoes volatiles show that more than 80% of He is derived from the mantle wedge and the contribution of volatiles from the subducting slab to He budget is low (Fischer et al. 1998; Hilton et al. 2002; Taran 2009). On the other hand, CO_2 and N_2, S, Cl and H_2O in arc magmas originate predominantly from the slab, i.e. from sediments and altered oceanic crust (AOC). All volatiles become coupled in the magma-generation zone and rise to the surface altogether in most cases as dissolved in magmas. Magma degassing in magma chambers or magmatic conduits may disturb the initial volatile composition due to different solubilities in magmas (Carroll and Webster 1994; Nuccio and Paonita 2001). N_2, Ar and He have low solubilities in silicate melts, comparable within one order of magnitude, (Nuccio and Paonita 2001; Miyazaki et al. 2004) and have low (N_2) or no (Ar, He) reactivity. Therefore they remain almost coupled until the surface. CO_2 has also low solubility in magmas, lower than that of HCl, H_2O and sulfur (Carroll and Webster 1994). Moreover, these components have also low solubility in water and therefore will not be affected by the condensation of volcanic vapor at shallow levels. If the predominant source of He, CO_2, Ar and N_2 is magma, the corresponding volcanic gases must demonstrate a simple mixing trend between almost zero-He, Ar, N_2 and CO_2 air-saturated water vapor and a parent magmatic gas composition. A set of diagrams with different species plotted vs He is shown in Fig. 9. Very good positive correlations with He can be seen for CO_2 and N_2 and not so good but still doubtless for other components except the total sulfur. CO_2-He and N_2-He data points show a mixing between almost zero-N_2 and CO_2 meteoric endmember and an endmember with N_2/He close to 2400 and CO_2/He ~1.6×

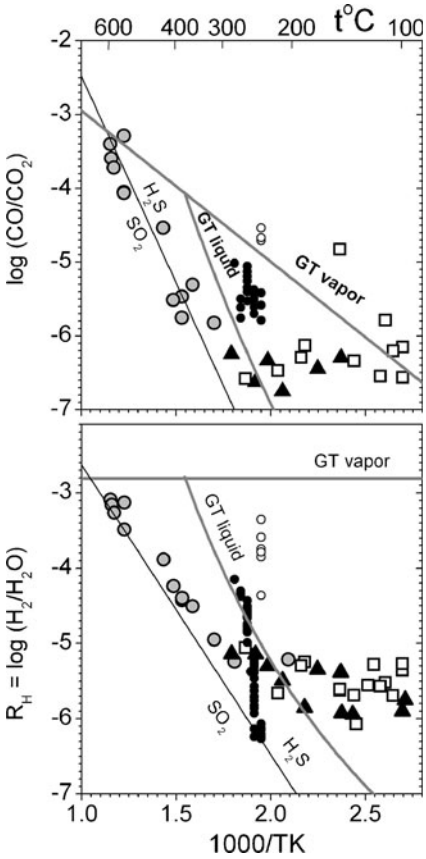

Fig. 5 Redox-diagrams for gases from the Mutnovsky crater in terms of log (CO/CO_2) vs temperature and R_H = log (X_{H2}/X_{H2O}) vs temperature. Lines for the "rock" buffer (GT vapor and GT liquid) and "gas" buffer (H_2S-SO_2) are plotted according to Giggenbach (1987, 1992). For symbols see Fig. 3

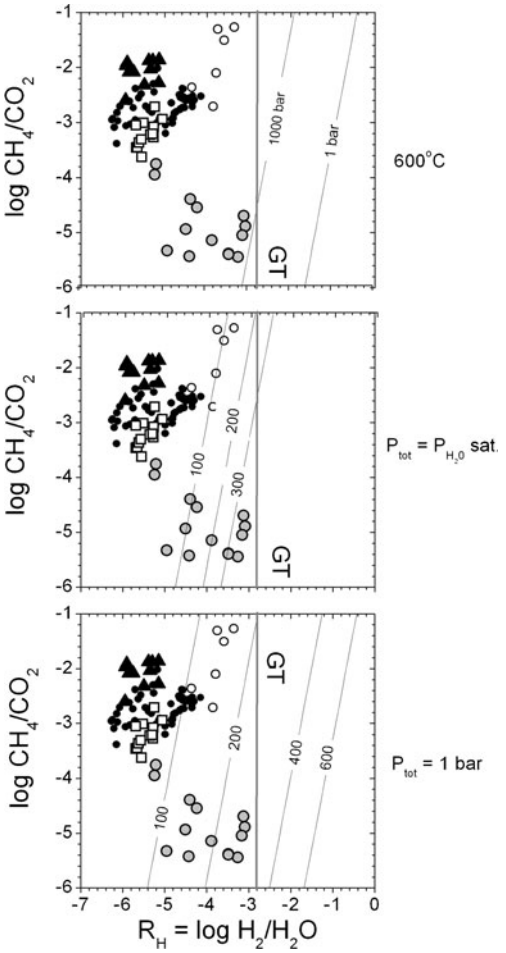

Fig. 6 Variations in X_{CH4}/X_{CO2} in volcanic and hydrothermal gases of Mutnovsky as a function of discharge temperature. Lines of full equilibrium for different pressures at 600°C (up); Equilibrium lines for different temperatures at saturation pressure (middle); Equilibrium lines for different temperatures at 1 atm pressure. GT line (R_H=−2.81) corresponds to the "rock" buffer (Giggenbach, 1987; Taran and Giggenbach, 2003). For symbols see Fig. 3

10^5. Despite Cl, δD and $\delta^{18}O$ can be affected by deep and shallow processes of magma degassing, dissolution in groundwater and elemental and isotopic fractionation in processes of phase separation (crystallization, boiling), their correlation with He also indicates that a high He concentration in the volcanic gas is associated with a high Cl content and the enrichment of water vapor with heavy isotopes. There is no correlation of He with sulfur, as well as sulfur with other species (except CO_2 in AF gases, Fig. 4), indicating a high mobility of sulfur in shallow processes like precipitation of native S and remobilization from previous precipitates and incrustations in fimarolic conduits (Giggenbach 1987; Taran et al. 1992; Chiodini et al. 1993).

The main feature of volcanic gases of Mutnovsky is that three separated in space fumarolic fields located within the same volcano edifice discharge gases with different and apparently "incompatible" compositions—they do not lie on single mixing trends. The Upper Field fumaroles, in spite of their relatively high temperature (up to 280°C), discharge almost pure hydrothermal fluid with a very low fraction of magmatic components. The Bottom Field fumaroles probably affected by shallow boiling and condensation processes providing high variations in the chemical compositions of fluids. Though they apparently are a link between "hydrothermal" UF vents and "magmatic" AF fumaroles, their data points may have distinct slopes on N_2-He and CO_2-He plots (Fig. 9).

Mixing relationships for CO_2, N_2 and He for AF fumaroles that discharge more than 80% of the total gas output from Mutnovsky may be interpreted as the two-endmember mixing of meteoric-hydrothermal vapor and a magmatic component from a single source with CO_2/He and N_2/He ratios estimated from the slopes of the corresponding mixing trends. The Bottom Field fumaroles may be a mixture of the same meteoric hydrothermal component but with a fluid from another magmatic source. Active Funnel and Bottom Field may release gases from different, separated in space, magma chambers with different magma composition or different degree of degassing. It is supported also by

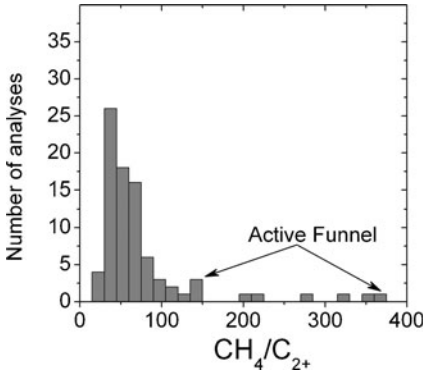

Fig. 7 Histogram showing distribution of CH_4/C_{2+} ratios in volcanic and hydrothermal gases of Mutnovsky. Mean value of 61 correspond to "thermogenic" origin of hydrocarbons. See text for discussion

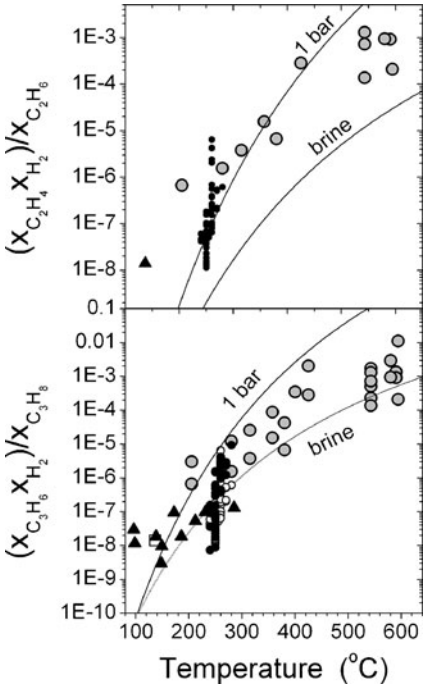

Fig. 8 Variations in the quotient ratios for reactions $C_2H_4 + H_2 = C_2H_6$ (upper panel) and $C_3H_6 + H_2 = C_3H_8$ (lower panel) as a function of discharge temperature for Mutnovsky volcanic and hydrothermal gases. The 1 bar equilibrium line corresponds to metastable equilibration under surface conditions. The "brine" line corresponds to vapors derived from a hypothetic saline brine with pressure controlled by the boiling of such a brine (Giggenbach 1987). For symbols see Fig. 3

the distinct N_2-Ar and He-Ar correlations shown in Fig. 10. The magmatic fluid source for the Active Funnel has N_2/He ~ 2400; N_2/Ar ~ 1000 and He/Ar ~ 0.4. The Bottom Field fumaroles are fed from a source with N_2/He ~ 1760; N_2/Ar ~ 370 and He/Ar ~ 0.2. The Upper Field gases are probably a mixture between BF mixed fumarolic gas and the same meteoric-hydrothermal fluid. CO_2 in BF fumaroles (Fig. 9) varies independently of He with large variations of CO_2/He. This can be caused by mixing of BF gases with a random amount of meteoric-hydrothermal fluid which has relatively high concentrations of CO_2, variable concentrations of N_2 and very low concentrations of He.

The parent magmatic gas

Good correlations between He and major species in AF hot gases may be used for the estimation of the composition of the parent magmatic gas feeding volcanic gases from AF. As it was outlined above, the isotopic composition of the parent gas may be approximated as $\delta D = -19‰$ and $\delta^{18}O = +5.9‰$ (see Fig. 11 for details). The latter value is the main reference point based on the rock isotopic composition (Bindeman et al. 2004) and an assumption that magmatic water has the same oxygen isotopic composition as the parent magmatic melt. The procedure of estimation of the composition of parent gas is shown in Fig. 12. He concentration in the magmatic component can be determined as 0.00022 mmol/mol from linear regression of the δD-He and $\delta^{18}O$-He correlations (Fig. 11b). Then, concentrations of H_2O, CO_2, N_2 and HCl can be determined by linear regression of the corresponding mixing relationships (Fig. 12). The composition of the parent gas is presented in Table 4 together with average compositions of fluids from BF and UF fields, steam vents and geothermal wells. Each component is done as a mean value with a corresponding standard deviation (1σ). Sulfur in the parent gas was calculated from the mass balance by the difference $1000–\Sigma C_i$ (mmol), where C_i are the estimated concentrations of other major components.

The Mutnovsky parent gas composition is different from the Kudryavy parent gas estimated by Taran et al. (1995) and Fischer et al. (1998) in H_2O, He, CO_2 and N_2 concentrations and almost identical to Kudryavy gas in S, Cl and Ar.

He isotopes in volcanic and hydrothermal gases of Mutnovsky

Three distinct fluid sources for fumaroles of Mutnovsky volcano (meteoric-hydrothermal, AF-source and BF-source) are in agreement with the presented and previous data on He-isotopes (Rozhkov and Verkhovsky 1990; Taran et al. 1992). Points with the highest absolute He concentration on the plot $^3He/^4He$ vs He concentration (Fig. 13) belong to the hottest AF gases and have $^3He/^4He$ values <6.6Ra, where $Ra = 1.39 \times 10^{-6}$, the air ratio. However, the highest $^3He/^4He$ of ~7.67Ra was observed in the Bottom Field fumaroles and the lowest values were measured in the Upper Field gases and fluids from hydrothermal vents and wells. Such a difference in He-isotope ratios for volcanic gases discharging from the same crater is difficult to explain taking into account that the Bottom Field gases, according to their chemical and water isotope compositions,

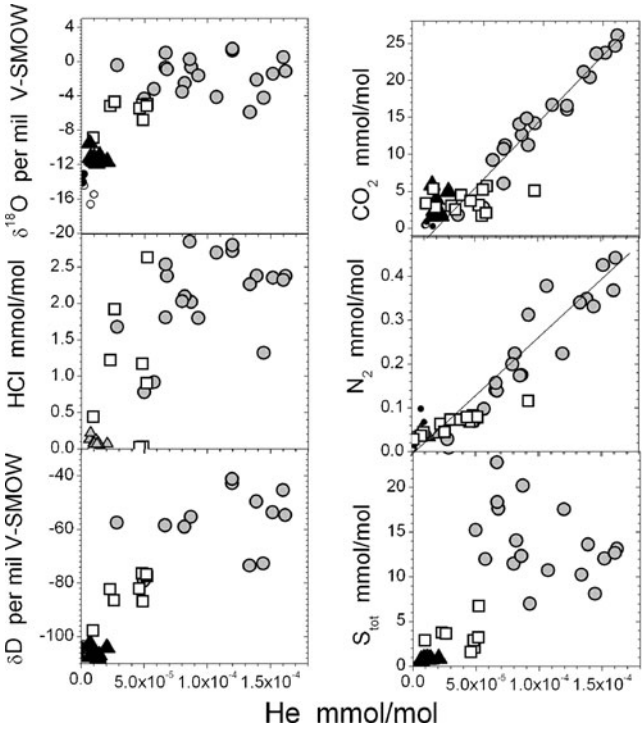

Fig. 9 Variations in water isotopes and major species in volcanic and hydrothermal gases of Mutnovsky as a function of He concentration. Lines show the apparently different mixing trends for AF and BF gases . For symbols see Fig. 3

are intermediate between almost "arc-magmatic", hot AF gases and "hydrothermal" UF gases.

Active Funnel with ~200 t/d of the permanent SO_2 flux is the orifice of magmatic conduit with a convecting magma, similar to other open-conduit volcanoes like White Island, Satsuma Iwojima, Kudryavy, (Giggenbach 1987; Kazahaya et al. 1994; Stevenson and Blake 1998; Botcharnikov et al. 2003). Discharge rate and composition of gases from AF do not vary significantly over the last 50 years. Relatively low $^3He/^4He$ ratios in AF gases may indicate that an intermediate, crustal magma chamber is the main contributor of magmatic fluids for the volcano, and some amount of radiogenic ^4He is admixed from the continental crust. Therefore, the Bottom Field fumaroles should be connected with another magma body with a much smaller or no contribution from the crustal fluid. Another possibility is that the observed $^3He/^4He$ ratios of the AF gases may not relate to the direct crustal contamination but to be a characteristic of the deep arc-magmatic fluid of this part of the Kamchatka arc.

All workers have noted a complicated nature of the Mutnovsky plumbing system and a large variety of the erupted products (Marenina 1956; Melekestsev et al. 1987; Selyangin 1993; Duggen et al. 2007). Duggen et al. (2007), based on the Pb-isotopes and trace elements study in lavas of Mutnovsky and the nearest Gorely volcanoes, found that some Mutnovsky volcanic front magmas are "polluted" with Gorely rear-arc melt component (with a higher fraction of the mantle material) due to specific conditions of the mantle wedge convection. It may be suggested, therefore, that a batch of this "polluted" magma is responsible for the high $^3He/^4He$ and lower N_2/Ar and N_2/He ratios in the Bottom Field fumaroles. Additionally, the Bottom Field may discharge gases from more degassed magmatic source than AF fumaroles. This may be supported by the ternary S_{tot}-CO_2-HCl plot (Fig. 3b) where AF and BF gases clearly demonstrate different S/Cl ratios and a relative enrichment of BF gases in Cl. Partially degassed magma is usually enriched in Cl, which is much more soluble than CO_2 and sulfur (Carroll and Webster 1994). The enrichment in Cl is accompanied with the depletion in deuterium of the releasing from magma water vapor (Villemant and Boudon 1999; Taran et al. 2002). However, we cannot prove this in our case due to a large scattering of the water isotopic composition of the Bottom Field fumaroles and a high proportion of meteoric vapor (Figs. 4 and 12). Moreover, the lower relative S content in BF fumaroles may be related to precipitation of native sulfur taking into account the lower temperatures compared with AF gas discharges.

Hydrothermal fluids from wells and steam vents are characterized by much lower He concentrations (He/Ar~ 0.005) but still high R/Ra of 4.5-5.5, typical for many other high-temperature hydrothermal systems with similar tec-

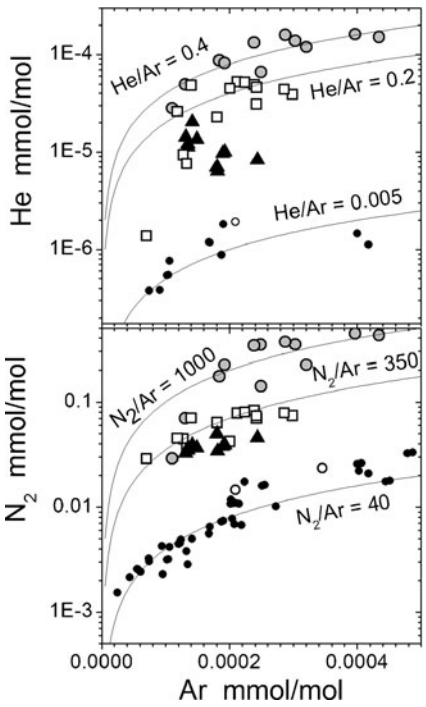

Fig. 10 Variations in N_2 and He in volcanic and hydrothermal gases of Mutnovsky as a function of their Ar content. Curves showing different He/Ar and N2/Ar are the regression lines for the corresponding clusters of points. Symbols as in Fig. 3

tonic setting. Fluids from geothermal wells of Mutnovsky as a rule are more depleted in ^{3}He than steam vents.

Nitrogen Isotopes

Table 2 shows a limited set of our data on nitrogen isotopes. All data are plotted in Fig. 14 against $N_{2,ex}$ where subscript "ex" stands for the fraction of excess nitrogen, i.e. non atmospheric N_2. The fraction of the non-atmospheric nitrogen in the samples can be estimated using $N_2/^{36}Ar$ ratio measured simultaneously with the N isotopic composition. (Inguaggiato et al. 2006). Two estimates of the fractions of non-atmospheric N_2 are shown in Table 2: one for the direct air contamination and another one for the ASW nitrogen. It can be seen that all hydrothermal gases are characterized by $N_2/^{36}Ar$ between the ASW value of 11200 and the air value of 24660. Therefore, values within this range have positive N excess relative ASW and negative one relative air (Table 2). Most of the hydrothermal samples have $\delta^{15}N$ close to zero.

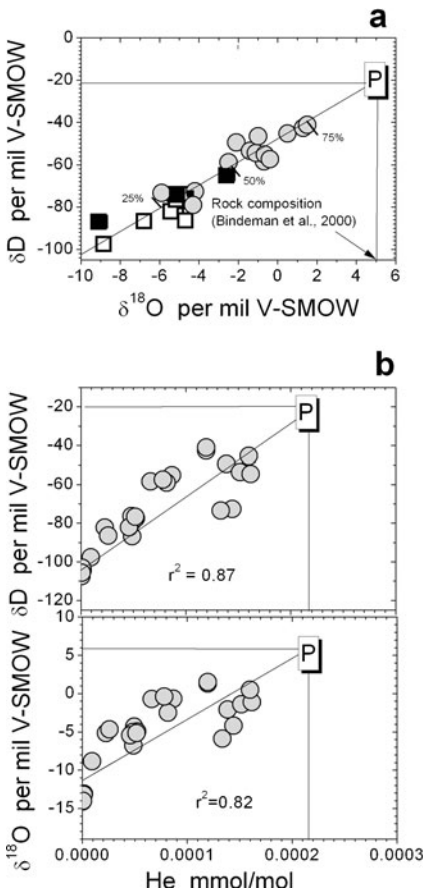

Fig. 11 **a** Evaluation of δD of the parent magmatic gas of Mutnovsky using extrapolation of data for Active Funnel and Bottom Field to the $\delta^{18}O$ value of +5.9‰ (average rock composition from Bindeman et al. 2004). **b** Evaluation of He concentration in the Mutnovsky parent gas (mmol/mol) using water isotopes. Black squares are BF data from Taran et al. (1992). Fractions of parent gas (%) are also shown on the panel (**a**). For other symbols see Fig. 3

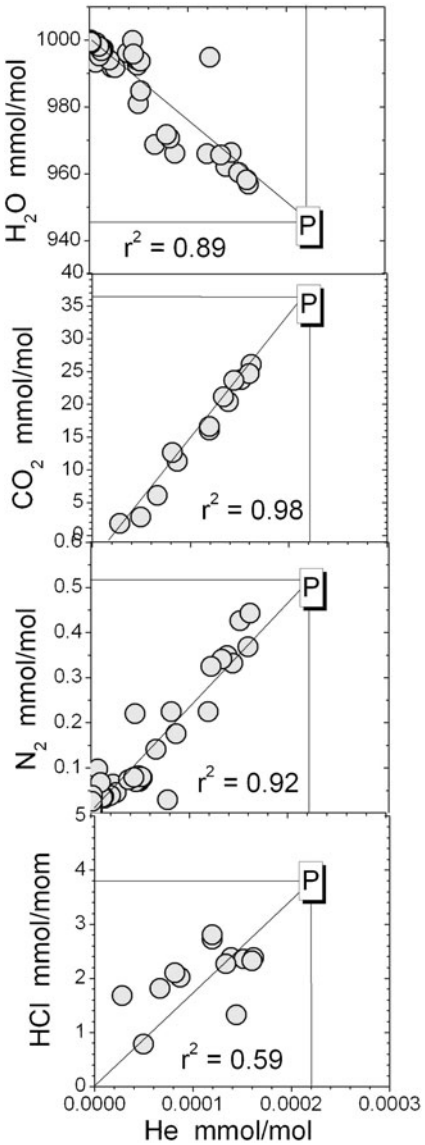

Fig. 12 Evaluation of the parent gas composition (CO_2, HCl, H_2O and N_2) using linear regression of their correlation with He

The Upper Field and Bottom field fumaroles in spite of high N_2/Ar (and $N_2/^{36}Ar$) have $\delta^{15}N$ also close to zero or slightly negative. One of geothermal wells (045) discharges N_2 with a negative $\delta^{15}N$ of −3.4‰. Li et al. (2009) reported a strong kinetic isotopic fractionation of N between NH_3 and N_2 with depletion of N_2 in ^{15}N relative NH_3 of ~35‰ at 600–700°C. It may be suggested that the NH_3/N_2 ratio is an important factor controlling $\delta^{15}N$ of N_2. Indeed, the NH_3/N_2 ratios shown in Table 2 are on average very low for AF, but close to 1 in the BF, UF and hydrothermal gases. The Active Funnel gases with the highest $N_2/^{36}Ar$ (and N_2/Ar) values have positive $\delta^{15}N$ with a tendency to have higher $\delta^{15}N$ in samples with a higher fraction of the non-atmospheric nitrogen. This is typical for many arc-type volcanoes and is considered to be a proof for the volatile contribution from the subducted

Table 4 Composition of parent gas (AF*) calculated for gases from the Active Funnel (see text for details) and mean compositions of gases from other sites. Concentrations in mmol/mol

	AF*	<BF>	<UF>	<SV>	<W>
H_2O	943	994±3	996±1.5	998.8±0.99	999.4
CO_2	36	3.72±1.32	2.89±1.42	1.16±0.9	0.53±0.27
HCl	3.2				
S_{tot}	17.2				
N_2	0.52	0.067±0.022	0.038±0.05	0.0595±0.035	0.016±0.014
Ar	5×10^{-4}	$(1.8\pm0.8)\times10^{-4}$	$(1.7\pm0.4)\times10^{-4}$	0.0011±0.0007	$(2.6\pm2.2)\times10^{-4}$
He	2.2×10^{-4}	$(3.8\pm2.3)\times10^{-5}$	$(1.1\pm0.4)\times10^{-5}$	$(5\pm3)\times10^{-6}$	$(1.1\pm0.5)\times10^{-6}$
CH_4	3×10^{-4}	0.0023±0.0007	0.022±0.003	0.011 ±0.006	0.0012±0.001
δD ‰	–19	–80.4±8.4	–106±1.8	–105 ±2	–105±2
δ18O ‰	+5.9	–5.6±1.8	–11.3±0.7	–15.5 ±1	–13.6±0.4
N_2/Ar	1040	372	224	54	62
N_2/He	2364	1763	3455	11900	14545
$^3He/^4He$ (R/Ra)	6.6	7.67	6.3	5.7	5.4
He/Ar	0.44	0.211	0.065	0.005	0.004
N_2/CH_4	1733	29.1	1.7	5.4	13.3
CO_2/N_2	62	56	76	19	33
CO_2/He	163636	97895	262727	232000	481818
$CO_2/^3He$	1.8×10^{10}	0.9×10^{10}	3×10^{10}	2.9×10^{10}	6.4×10^{10}
$N_2/^3He$	2.6×10^{8}	1.6×10^{8}	3.9×10^{8}	1.5×10^{9}	1.9×10^{9}
$Cl/^3He$	1.6×10^{9}	2.6×10^{9}	0.9×10^{9}	–	–

sediments (Sano et al. 2001; Fischer et al. 1998, 2002; Hilton et al. 2002; Inguaggiato et al. 2006; Inguaggiato et al. 2009).

Sources of the Mutnovsky gases

For arc volcanoes, several sources of fluid can be specified (e.g. Hilton et al. 2002; Wallace 2005; Taran 2009 and references therein). As the first approximation they are: upper mantle (MORB), subducted slab (S) and air saturated meteoric water (ASW). We do not take into account here air contamination during sampling or analysis. Main sources of volatiles from the subducted slab are oceanic sediments (SED) and a layer of altered oceanic basalts (AOC). An important source of volatiles may be the continental crust beneath the volcano edifice (CC). Altogether there are five endmembers (MORB-AOC-SED-CC-ASW) or four if an integrated slab endmember is considered (S = SED + AOC). We use the term "MORB" for the composition of the mantle in the mantle wedge and assume that this sub-arc astenospheric mantle has MORB characteristics in terms of volatile composition.

Table 5 shows mean elemental ratios and isotopic compositions of CO_2, N_2, Ar and He in main reservoirs, potential contributors of volatiles to volcanic gases of subduction zones. Characteristics of crustal gases (old metamorphic crust) are taken from KTB deep well in Germany (Bach et al. 1999; Lippmann et al. 2005). The only data on He and Ar for altered oceanic crust were reported by Staudacher and Allegre (1988). They have also reported the abundances of Ar and He in a few samples of pelagic oceanic sediments, isotopic compositions of Ar and He in altered basalts and only Ar isotopes in sediments. The published data on He abundances and isotopes in pelagic sediments (e.g. Ozima and Podosek 2002, for review) show very low He content and very high $^3He/^4He$ (30-100Ra) due to a constant (though at a very low rate) contribution from the cosmic dust (IDP—interplanetary dust particles). Hilton et al. (2002) have discussed the importance of these data for He balance in subduction zones and decided do not count this excess of ^3He in sediments referring to a probable loss of He from sediments before subduction by diffusion. Nitrogen in oceanic sediments and oceanic crust was analyzed by Sadofsky and Bebout (2004), Li and Bebout (2005), Li et al. (2007) and Busigny et al. (2005). The "Slab" component in Table 5 is presented as a mean composition with high N_2/Ar, N_2/He and a low $^3He/^4He$. A reason for this "averaging" is that it is impossible to distinguish contribution to N_2-Ar-He separately from sediments and AOC due to large uncertainties in Ar and He concentrations.

Two plots (modified from Taran 2009) with mixing lines between main potential reservoirs of N_2, Ar and He are shown in Fig. 15. The point for the evaluated parent gas (AF) is very close to the mixing lines between slab and mantle. Other points for volcanic gases (BF and UF) are shifted to the mantle-atmosphere mixing lines. Hydrothermal gases occupy positions closer to the mantle-atmosphere mixing lines.

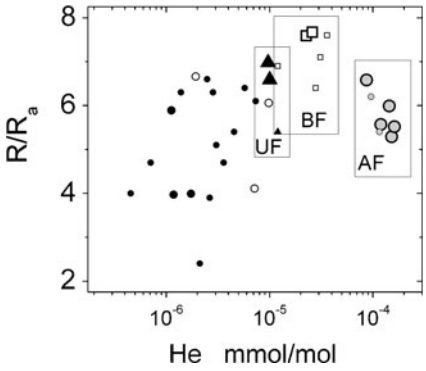

Fig. 13 Helium isotopic composition as a function of He concentration in gases of Mutnovsky. Small symbols are from Taran et al. (1986) and Rozhkov and Verkhovsky (1990)

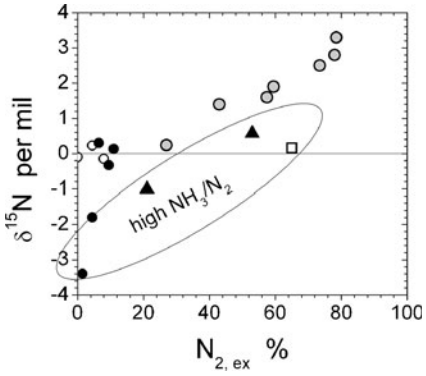

Fig. 14 Isotopic composition of nitrogen as a function of excess N_2 calculated from the $N_2/^{36}Ar$ ratio relative ASW (Table 2). See text for explanation. Symbols as in Fig. 3

Distinguishing between various sources of volatiles (mantle wedge, subducted slab, sub-arc crust) is possible by considering the four coupled components (CO_2, N_2, Ar, He) altogether. In that case the concentration of each component of the parent magmatic gas X_i is a weighed sum

$$X_i = \sum f_j X_{ij}, \quad (1)$$

where f_j is the fraction of fluid from each source (endmember) and X_{ij} is the concentration of each specie normalized by the sum CO_2 + N_2 + Ar + He. If there are four sources (reservoirs): M- mantle; S—slab; C—crust, and A—atmosphere (ASW), then we have four equations for four variables. Taking into account the mass balance equation $f_M + f_S + f_C + f_A = 1$, we can use three equations for concentrations and one for the mass balance. This approach is considered in details by Albarede (1995). If all parameters are chosen correctly, the solution (f_j) of the system with the observed or presumed composition of the parent (or any) gas X_i is a set of f_j values with $0 \le f_j \le 1$. This solution should be the same for any set of three equations for concentrations, for example, (CO_2, He, Ar), (CO_2, N_2, He), (N_2, He, Ar), etc. In practice, all parameters (concentrations) of endmembers are mean values with large standard deviations. Moreover, the slab endmember in terms of CO_2 + N_2 + Ar + He is poorly determined because of the unknown fraction of carbon subducted to the lower mantle (Kerrick and Connoly 2000; Poli and Schmidt 2002). The observed or presumed gas compositions at the surface have also certain errors or ranges of values. Therefore, this "ideal" approach for the system (CO_2-N_2-Ar-He) does not work, giving either different reasonable solutions for different sets of equations or solutions that do not make sense (f_j negative and/or >1). Nevertheless, the set of endmember compositions presented in Table 5 for the N_2-Ar-^{4}He-^{3}He mixture (CO_2 is replaced for ^{3}He) is "compatible" with any composition of Mutnovsky gases shown in Table 4. This means that any combination of equations: N_2-Ar-^{4}He, N_2-^{4}He-^{3}He, Ar-^{4}He-^{3}He, N_2-Ar-^{3}He-^{4}He—derives almost identical solutions (f_i) for a given composition of the gas. Table 6 shows fractional contributions to the N_2-Ar-He system of Mutnovsky gases from mantle, slab, continental crust and air-saturated water calculated by using this method. Only ~1% (mole basis) of the N_2+ Ar + He mixture enter to the parent Mutnovsky gas from the mantle wedge. But this 1% of N_2 + He + Ar carrying almost 1% of the mantle N_2, contains more than 80% of the total mantle He and more than 95% of the total ^{3}He. The predominant contribution of N_2 (>95%) occurred from the slab. The contribution from the crust beneath the volcano is negligible. However, even the "corrected" parent gas composition has a fraction (~3%) of ASW. The ASW fraction increases from parent gas to hydrothermal gases from steam vents and wells where it reaches more than 60%.

A system including CO_2 and carbon isotopic composition is needed to distinguish contributions from subducted sediments and oceanic crust. In a three end-member model consisting of MORB (M), slab-derived marine carbonate (L) and organic carbon (S) used by a number of authors (Hilton et al. 2002; Shaw et al. 2003 and references therein), carbon isotopic composition of CO_2 and $CO_2/^3$He are the most popular parameters for estimations of the fraction contributed from each reservoir. The following mass balance equations were first used by Sano and Marty (1995):

$$\delta^{13}C_o = f_M\delta^{13}C_M + f_L\delta^{13}C_L + f_S\delta^{13}C_S \quad (2)$$

$$\left(^3He/CO_2\right)_o = f_M\left(^3He/CO_2\right) + f_L\left(^3He/CO_2\right) + f_S\left(^3He/CO_2\right) \quad (3)$$

$$f_M + f_L + f_S = 1 \quad (4)$$

This approach is fruitful for the Kamchatkan gases because subducting oceanic sediments close to the Kamchatka trench do not contain carbonates (Plank and Langmuir 1998; Hilton et al. 2002; Jarrard 2003). Therefore, it can be suggested that all carbonate carbon contributing to magmatic gases of

Table 5 Relative concentrations and isotopic compositions of N_2, Ar and He in different terrestrial reservoirs, potential contributors to the subduction–type magmas, in parent gas of Mutnovsky and in some subduction–related volcanic gases. Vulcano M corresponds to magmatic component in gases as defined by Taran (2011). The uncertainties (relative errors) are given very approximately, just to give an idea about the natural scatter of data. Error of 100% indicates that the observed variations may be higher than one order of magnitude

Reservoir	N_2/Ar	N_2/He	He/Ar	R/Ra	$N_2/^3$He	CO_2/N_2	CO_2/He	Error %	Ref
MORB	100	25	4	8	2.3E+08	1000	2.2E+04	30	1–3
AOC	10000	20000	0.5	0.1	1.4E+11	60	1E+06	100	3,4
SED	40000	2E+05	0.2	??	2.2E+11	60	1E+07	100	3,4
KTB	700	100	7	0.07	4.2E+09	0.00033	0.035	30	5,6
Mutnovsky P	1040	2364	0.44	6.59	1.9E+08	69	1.8E+05	20	7
Kudriavy P	380	2100	0.18	6.70	2.2E+08	72	1.5E+05	50	8
Vulcano M	470	470	1	6.2	5.4E+07	140	6.7E+04	50	9
Air	83.6	1.49E+05	5.61E–04	1	1.1E+11	0.00045	67		
ASW 5°C	38	2.64E+05	1.46E–04	1	1.9E+10	0.015	1000		

References: 1– Marty and Humbert (1997); 2—Marty and Zimmermann (1999); 3—Hilton et al. (2002); 4—Staudacher and Allegre (1988); 5—Bach et al. (1999); 6—Lippmann et al. (2005); 7—this work; 8—Fischer et al. (1998); 9—Taran (2011)

Mutnovsky is derived from the oceanic crust (AOC), and all organic fraction is derived from oceanic sediments. The only data on $\delta^{13}C$ of CO_2 in Mutnovsky gases were published by Taran (1988) for the hydrothermal system and Taran et al. (1992) for crater fumaroles. A mean value for $\delta^{13}C$-CO_2 of all Mutnovsky gases may be estimated as −9±2‰ (V-PDB), i.e. they are relatively enriched in ^{12}C compared with the mantle values in the −5‰ to −7‰ range (e.g. Javoy et al. 1986). Relatively isotopically light CO_2 is common for Kamchatkan volcanoes (Taran 1992) and for volcanoes from some other subduction zones like Cascadian and New Zealand (Taylor 1986).

We accept $CO_2/^3$He ratios of 2×10^9, 1×10^{13} and 1×10^{13} for M, L and S, respectively, from Hilton et al. (2002). For $\delta^{13}C$ of organic carbon a value of −25‰ is accepted. Solution of the system (2–4) for the parent Mutnovsky gas with $\delta^{13}C$-CO_2 = −9‰ and $CO_2/^3He=2\times10^{-10}$ (Table 3) gives M=0.1; S=0.4 and L=0.5. In this case the mantle contribution of CO_2 is ~10 times higher than that of N_2 compared with the N_2-Ar-He system. This result is in a qualitative agreement with conclusions of Taran (2009) who estimated the mantle contribution of CO_2 to Kamchatkan magmatic fluids as 18% and N_2 as ~3% (mole basis). Fischer et al. (1998) estimated 12% of the mantle CO_2 and 2% of the mantle N_2 for Kudryavy gases which is very close to our values for Mutnovsky. Application of the method to BF gases gives a much higher mantle contribution for CO_2 (32%) and same L/S (or AOC/Sed) ratio. This result together with a significantly higher $^3He/^4He$ in BF fluids may indicate the presence of a separate degassing magma body for the Bottom Field fumaroles. Application of the method to UF volcanic gases and hydrothermal gases does not make much sense because UF gases are strongly affected by hydrothermal fluids, and CO_2 in hydrothermal fluids is controlled by thermodynamic conditions of the hydrothermal aquifer (Giggenbach 1980, 1997b; Taran 1986).

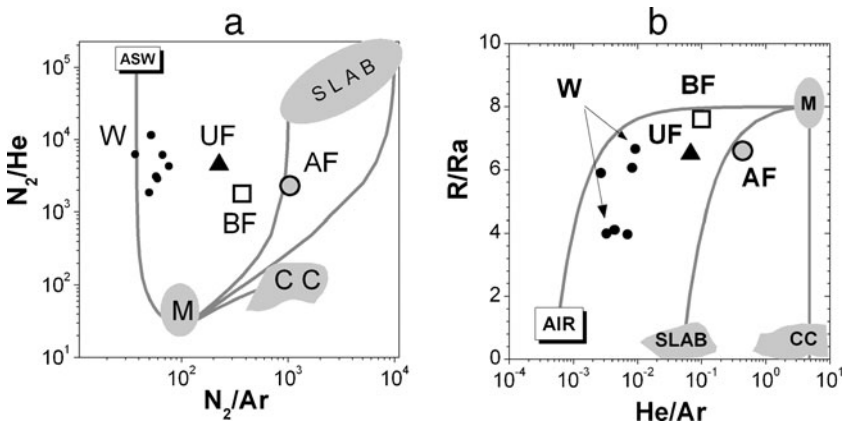

Fig. 15 Plots N_2/He vs N_2/Ar (**a**) and R/Ra vs He/Ar (**b**) for volcanic and hydrothermal gases of Mutnovsky. Shaded areas approximately correspond to compositional variations of end-members. Point AF is plotted as for the parent gas with the extracted meteoric component (Table 4). Points UF and BF are mean values for the compositions of gases from UF and BF (Table 4)

Table 6 Fractional contributions of MORB (M), slab (S), continental crust (C) and atmosphere (A) to N_2, Ar and He in volcanic and hydrothermal gases of Mutnovsky. The fractions are obtained as a solution of equations (1) with different sets of species. AF* parent gas

	AF*	<BF>	<UF>	<SV>	<W>
	N_2+He+Ar				
M	0.01	0.014	0.007	0.0001	0.001
S	0.96	0.89	0.83	0.297	0.39
C	0.00013	0.0025	0.0003	0.014	0
A	0.031	0.095	0.17	0.69	0.61
	N_2+^{3}He+^{4}He				
M	0.0091	0.014	0.0059	0.0015	0.001
S	0.96	0.89	0.82	0.306	0.39
C	0.0052	0.00014	0.0042	0.0017	0.0013
A	0.031	0.095	0.17	0.69	0.61
	N_2+Ar+^{4}He+^{3}He				
M	0.0091	0.014	0.0059	0.0015	0.0011
S	0.90	0.88	0.81	0.25	0.34
C	0.0053	0	0.004	0.0018	0.0014
A	0.085	0.10	0.18	0.75	0.66
	Ar+^{4}He+^{3}He				
M	0.0091	0.014	0.0059	0.0015	0.0011
S	0.90	0.73	0.54	0.25	0.34
C	0.0053	0	0.005	0.0018	0.0015
A	0.085	0.26	0.45	0.75	0.66

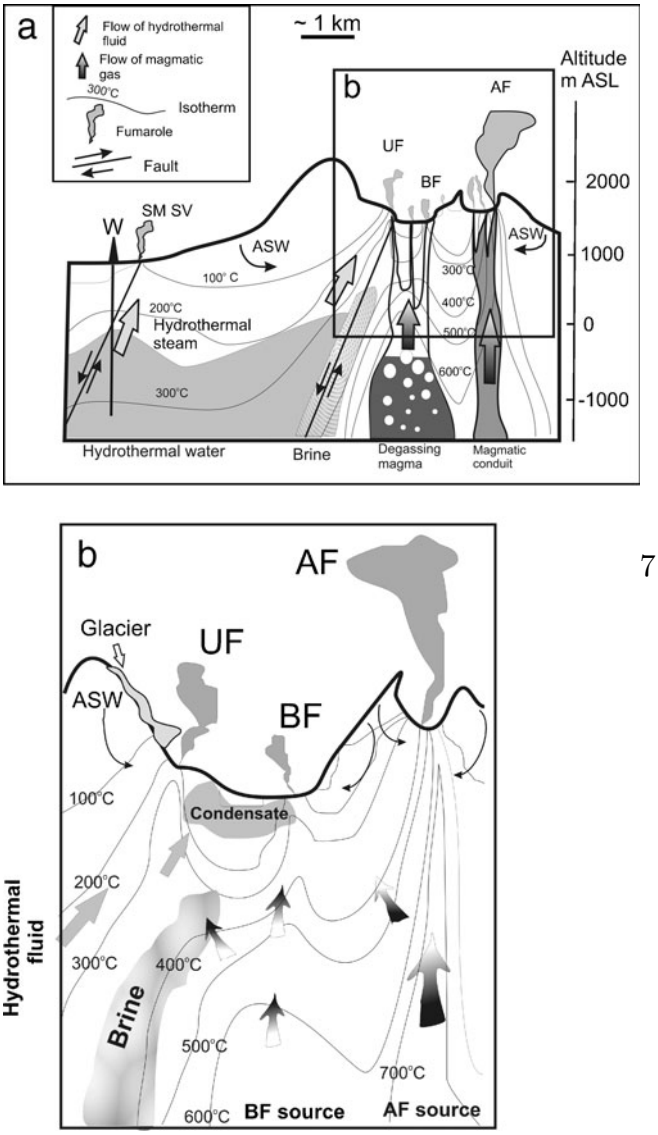

Fig. 16 **a** A conceptual model of the volcano-hydrothermal system of Mutnovsky. A cross-section is drawn through Mutnovsky crater (appx SW-NE) and the Mutnovsky edifice (appx N-S) showing temperature distribution and main fluid flows. **b** Fluid flows and temperature distribution beneath the crater. AF, BF, UF are Active Funnel, Bottom and Upper Fields, respectively. SM-SV denotes "Severo-Mutnovsky steam vents", W—geothermal well

Concluding Remarks

(1) To provide the existing compositional and thermal distribution of fumarole discharges at Mutnovsky, there must be at least three independent deep sources of fluid: (1) a large source of magma with a continous high flux of volatiles (80% of the total flux) through the open conduit of the Active Funnel; (2) a distinct magma body with higher ^{3}He/^{4}He , lower CO_2/^{3}He and N_2/^{3}He feeding the Bottom Field; (3) a high-temperature hydrothermal fluid with a high CH_4 content, which is the predominant source for the Upper Field gases. These sources of fluids are schematically shown in Fig. 16 on the hypothetical North-South cross-section of the volcanic edifice and the adjacent hydrothermal aquifer of Mutnovsky.

(2) The Active Funnel emits the hottest and most concentrated gas that requires a hot convecting magma body. Its parent magmatic gas characteristics are typical of a subduction-related magmatic gas, with the main volatile contribution from the subducted slab. This magma body must be of significant size. Taran et al. (1992) have estimated the volume of the completely degassed melt necessary to ensure the observed emission rate at ~4 km^3 per 100 years. It is not clear whether this magma chamber is related to a large intrusive body whose presence beneath the volcano and hydrothermal system has been deduced from results of the geophysical survey (Selyangin and Ponomareva 1999).

(3) The Bottom Field is probably fed from a separate magma body whose volatile characteristics are more similar to those of rear-arc magmas with a larger contribution of volatiles from the mantle wedge. It is likely to be a shallow intrusive body of crystallizing basaltic magma responsible for the last basaltic eruptions of Mutnovsky and "contaminated" by the

rear-arc component as suggested by Duggen et al. (2007). Fumarolic gases of the Bottom Field are influenced by shallow hydrothermal processes because of the existence of a liquid phase (brine?) beneath the crater (Fig. 16b). This liquid phase is most probably a partially evaporated mixture of the volcanic gas condensate with meteoric water and the condensate of hydrothermal steam feeding the Upper field fumaroles. Subsurface boiling of this highly acidic condensate may provide a wide range of HCl and S concentrations in volcanic vapors and strong variations in the vapor isotopic compositions.

(4) The mixed fluid venting through the Upper Field is most probably controlled by a fault, contains only <2% of the parent magmatic gas and is composed of hydrothermal fluid. A notable feature of the Upper Field hydrothermal gas is an elevated CH_4 content which is higher than in the fluid of the main geothermal field. The high-CH_4 volcanic-hydrothermal fluid discharging from the Upper Field fumaroles may partially represent a secondary component, a vapor derived from a deep, two-phase, saline brine-vapor "envelope" formed near the contact between hydrothermal aquifer and the magmatic system of Mutnovsky, similar to what has been suggested by Giggenbach (1987) for White Island.

(5) The nearest hydrothermal manifestations northward of Mutnovsky are separated by a distance of 5 km from the crater fumarole fields (Fig. 2). They are very similar to the UF gases in terms of the isotopic composition of water vapor, with the difference in the ^{18}O shift and a lower CH_4 concentration. Three main features of the UF gases are not simple to explain: (1) their elevated methane content which is higher than in hydrothermal fluid from steam vents and wells; (2) a high fraction of non-atmospheric nitrogen (N_2/Ar~230); (3) the high temperature of fumaroles, up to 280°C, that requires an additional heat source to maintain the temperature of the deep hydrothermal fluid to the surface. The heat problem might be resolved assuming that the heat source can be the same shallow basaltic intrusion beneath the main crater, which is the source of BF gases (Fig. 16). We speculate that the excess CH_4 and non-atmospheric N_2 are derived from a non-magmatic source at the interface between the magmatic and hydrothermal system (hydrothermal "envelope"), most probably from the deeper part of the volcano-hydrothermal system. On the other hand, ~2% of the parent gas or ~12% of the BF gas added to hydrothermal fluid represented by SV gases can provide the required N_2/Ar ratio for UF gases. In this case the non-atmospheric N_2 and CH_4 have different sources (magmatic and crustal).

Acknowledgements This study was partly supported by a grant from the Russian Foundation of Basic Research # 07-05-552. The authors thank Andrea Rizzo, Fausto Grassa, Giorgio Capasso, Edith Cienfuegos, Boris Pokrovsky, Elena Dubinina for providing isotope analyses and Slava Shapar for GC analyses. Tobias Fischer is thanked for the permission to use his unpublished data on the SO_2 flux. Constructive reviews by Mauro Martelli and Andrea Rizzo are greatly acknowledged. Many thanks to John Stix for his patience when editing the last version of the manuscript.

References

Albarede F (1995) Introduction to geochemical modeling. Cambridge University Press, Cambridge

Andres RJ, Kasgnoc AD (1998) A time-averaged inventory of subaerial volcanic sulfur emissions. J Geophys Res 103:25,251–25,261

Arutyunov AS, Krylov BI (1998) Oxidative conversion of methane. Nauka, Moscow

Bach W, Naumann D, Erzinger J (1999) Helium, argon and nitrogen of the upper continental crust (KTB drill holes, Oberpfalz, Germany): implications for crustal degassing. Chem Geol 160:81–101

Bindeman IN, Ponomareva VV, Bailey JC, Valley JW (2004) Volcanic arc of Kamchatka: a province with high-$\delta^{18}O$ magma source and large-scale $^{18}O/^{16}O$ depletion of the upper crust. Geochim Cosmochim Acta 68:841–865

Botcharnikov RE, Shmulovich KI, Tkachenko SI, Korzhinsky MA, Rubin AV (2003) Hydrogen isotope geochemistry and heat balance of a fumarolic system: Kudryavy volcano, Kuriles. J Volcanol Geotherm Res 118:1–22

Busigny V, Laverne C, Bonifacie M (2005) Nitrogen content and isotopic composition of oceanic crust at a superfast spreading ridge: a profile in altered basalts from ODP Site 1256, Leg 206. Geochem Geophys Geosyst 6: Q12O01. doi:10.1029/2005GC001020

Carroll MR, Webster JD (1994) Solubilities of sulfur, noble gases, nitrogen, chlorine and fluorine in magmas. In: Carrol MR, Holloway JC (eds) Volatiles in magmas. Rev Mineral 30:67–100

Cheshko AL, Esikov AD (1990) Deuterium and ^{18}O in groundwaters and precipitations of Kamchatka and Kuril islands. Water Res 6:121–129 (in Russian)

Chiodini G, Marini L (1998) Hydrothermal gas equilibria: the H_2O-H_2-CO_2-CO-CH_4 system. Geochim Cosmochim Acta 62:2673–2687

Chiodini G, Cioni R, Marini L (1993) Reactions governing the chemistry of crater fumaroles from Vulcano Island, Italy, and implications for volcanic surveillance. Appl Geochem 8:357–371

Craig H (1961) Isotopic variations in meteoric waters. Science 133:1702–1703

Duggen S, Portnyagin M, Baker J, Ulfbek D, Hoernle K, Garbe-Schonberg D, Grassineau N (2007) Drastic shift in lava geochemistry in the volcanic front to rear-arc region of the Southern Kamchatkan subduction zone: Evidence for the transition from slab surface dehydration to sediment melting. Geochim Cosmochim Acta 71:452–480

Fischer TP (2008) Fluxes of volatiles (H_2O, CO_2, N_2, Cl, F) from arc volcanoes. Geochem J 42:21–38

Fischer TP, Giggenbach WF, Sano Y, Williams SN (1998) Fluxes and sources of volatiles discharged from Kudryavy, a subduction zone volcano, Kurile Islands. Earth Planet Sci Lett 160:81–96

Fischer TP, Hilton DR, Zimmer MM, Shaw AM, Sharp ZD, Walker JA (2002) Subduction and recycling of nitrogen along the Central American margin. Science 297:1154–1157

Giggenbach WF (1975) A simple method for the collection and analysis of volcanic gas samples. Bull Volcanol 39:15–27

Giggenbach WF (1980) Geothermal gas equilibria. Geochim Cosmochim Acta 44:2021–2032
Giggenbach WF (1987) Redox processes governing the chemistry of fumarolic gas discharges from White Island, New Zealand. Appl Geochem 2:143–161
Giggenbach WF (1992a) The composition of gases in geothermal and volcanic systems as a function of tectonic setting. Proc Int Symp Water-Rock Interaction WRI-8 873–878
Giggenbach WF (1992b) Isotopic shift in waters from geothermal and volcanic systems along convergent plate boundaries and their origin. Earth Planet Sci Lett 113:495–510
Giggenbach WF (1997a) Relative importance of thermodynamic and kinetic processes in governing the chemical and isotopic composition of carbon gases in high-heatflow sedimentary basins. Geochim Cosmochim Acta 61:3763–3785
Giggenbach WF (1997b) The origin and evolution of fluids in magmatic-hydrothermal systems. In: Barnes HL (ed) Geochemistry of hydrothermal ore deposits. Wiley, NY, pp 737–796
Gorbatov A, Kostoglodov V, Suarez G, Gordeev E (1997) Seismicity and structure of the Kamchatka subduction zone. J Geophys Res 102:17883–17898
Hilton DR, Fischer TP, Marty B (2002) Noble gases and volatile recycling at subduction zones. In: Porcelli D, Ballentine CJ, Wieler R (eds) Noble gases in cosmochemistry and geochemistry. Rev Mineral 47:319–370
Hochstein MP, Bromley CJ (2001) Steam cloud characteristics and heat output of fumaroles. Geothermics 30:547–559
Horita J, Wesolowski DJ (1994) Liquid-vapor fractionation of oxygen and hydrogen isotopes of water from the freezing to the critical temperature. Geochim Cosmochim Acta 58:3425–3437
Inguaggiato S, Grassa F, Capasso G, Favara R, Rizzo A, Taran Y (2006) Simultaneous determination of ^{36}Ar and N_2 content together with $\delta^{15}N$ values in gas samples: examples from different arc-related volcanic systems. AGU Fall Meeting 2006 V33A-0638
Inguaggiato S, Taran YA, Fridriksson T, Melian G, D'Alessandro W (2009) Nitrogen isotopes in volcanic fluids of different tectonic settings. Geochim Cosmochim Acta 73:A571
Jarrard RD (2003) Subduction fluxes of water, carbon dioxide, chlorine and potassium. Geochem Geophys Geosys 4:U1–U50. doi:10.1029/2002GC000392
Javoy M, Pineau F, Delorm H (1986) Carbon and nitrogen isotopes in the mantle. Chem Geol 57:41–62
Kazahaya K, Shinohara H, Saito G (1994) Excessive degassing of Izu-Oshima volcano: magma convection in a conduit. Bull Volcanol 56:207–216
Kerrick DM, Connoly JAD (2000) Metamorphic devolatilization of subducted oceanic metabasalts: implications for seismicity, arc magmatism and volatile recycling. Earth Planet Sci Lett 189:19–29
Kirsanov IT (1964) The state of active volcanoes in Middle and Southern Kamchatka in 1961–1962. Bull Volcanol Stations 36:48–60 (in Russian)
Li L, Bebout GE (2005) Carbon and nitrogen geochemistry of sediments in the Central American convergent margin: Insights regarding subduction input fluxes, diagenesis, and paleoproductivity. J Geophys Res 110:B11202. doi:10.1029/2004JB003276
Li L, Bebout GE, Ildelman BD (2007) Nitrogen concentration and $\delta^{15}N$ of altered oceanic crust obtained on ODP Legs 129 and 185: insight into alteration-related nitrogen enrichment and the nitrogen subduction budget. Geochim Cosmochim Acta 71:2344–2360
Li L, Cartigny P, Ader M (2009) Kinetic nitrogen-isotope fractionation associated with thermal decomposition of NH_3. Experimental results and potential application to trace the origin of N_2 in natural gas and hydrothermal systems. Geochim Cosmochim Acta 73:6282–6297
Lippmann J, Erzinger J, Zimmer M, Schloemer S, Eichinger JL, Faber E (2005) On the geochemistry of gases and noble gas isotopes (including ^{222}Rn) in deep crustal fluids. The 4000 m KTB-pilot hole fluid production test 2002/03. Geofluids 5:52–66
Marenina TY (1956) Geological and petrographical sketch of Mutnovsky volcano. Proceed Lab Volcanol SSSR Acad Sci 12:1–124 (in Russian)
Marty B, Humbert F (1997) Nitrogen and argon isotopes in oceanic basalts. Earth Planet Sci Lett 152:101–112
Marty B, Zimmermann L (1999) Volatiles (He, C, N, Ar) in mid-ocean ridge basalts: assessment of shallow-level fractionation and characterization of source composition. Geochim Cosmochim Acta 63:3619–3633
Mather TA, Pyle DM, Tsanev VI, McGonigle AJS, Oppenheimer C, Allen AG (2006) A reassessment of current volcanic emissions from the Central American arc with specific examples from Nicaragua. J Volcanol Geotherm Res 149:297–311
Melekestsev IV, Braitseva OK, Ponomareva VV (1987) Dynamics of activity of Mutnovsky and Gorely volcanoes in Holocene and potential hazard for adjacent regions. Volcanol Seismol 3:3–18 (in Russian)
Miyazaki A, Hiyagon H, Sugiura H, Hirose K, Takahasi E (2004) Solubilities of nitrogen and noble gases in silicate melts under various oxygen fugacities: Implications for the origin and degassing history of nitrogen and noble gases in the Earth. Geochim Cosmochim Acta 68:387–401
Muraviev AV, Polyak GB, Turkov VP, Kozlovtseva SV (1983) New estimation of heat output with fumarolic activity from Mutnovsky volcano (Kamchatka). Volcanol Seismol 5:51–63, in Russian
Nuccio PM, Paonita A (2001) Magmatic degassing of multicomponent vapors and assessment of magma depth: application to Vulcano Island (Italy). Earth Planet Sci Lett 193:467–481
Ozima M, Podosek FA (2002) Noble gas geochemistry. Cambridge University Press, Cambridge
Plank T, Langmuir CH (1998) The chemical composition of subducting sediments and its consequences for the crust and the mantle. Chem Geol 145:325–394
Poli S, Schmidt MW (2002) Petrology of subducted slabs. Ann Rev Earth Sci 30:207–235
Polyak BG, Bezukh BA, Kaftan VI (1985) Terrestrial infrared survey for evaluation of temperature and heat radiation from thermal fields of Mutnovsky volcano. Volcanol Seismol 5:86–95
Rozhkov AM, Verkhovsky AB (1990) Geochemistry of noble gases in high temperature hydrothermal systems. Moscow, Nauka (in Russian)
Sadofsky SJ, Bebout GE (2004) Nitrogen geochemistry of subducting sediments: new results from Izu-Bonin-Marianamargin. Geochem Geophys Geosys 5:Q03115. doi:10.1029/2003GC000543
Sakai H, Matsubaya O (1977) Stable isotope studies of Japanese geothermal systems. Geothermics 5:97–124
Sano Y, Marty B (1995) Origin of carbon in fumarolic gas from island arcs. Chem Geol 119:265–274
Sano Y, Wakita H (1985) Geographical distribution of $^3He/^4He$ in Japan: implications for arc tectonics and incipient magmatism. J Geophys Res 90:8729–8741
Sano Y, Takahata N, Nishio Y, Marty B (1998) Nitrogen recycling in subduction zones. Geophys Res Lett 25:2289–2292
Sano Y, Naoto T, Nishio Y, Fischer TP, Williams SN (2001) Volcanic flux of nitrogen from the Earth. Chem Geol 171:263–271
Selyangin OB (1993) New data on Mutnovsky volcano: structure, evolution and prediction. Volcanol Seismol 1:17–35 (in Russian)
Selyangin OB, Ponomareva VV (1999) Gorelovsky volcanic center, Southern Kamchatka: structure and evolution. Volcanol Seismol 2:3–23 (in Russian)
Serafimova EK (1966) Chemical composition of fumarolic gases at Mutnovsky volcano. Bull Volcanol Stations 42:56–65 (in Russian)
Shaw AM, Hilton D, Fischer TP, Walker JA, Alvarado GE (2003) Contrasting He-C relationship in Nicaragua and Costa Rica: insights into C cycling through subduction zones. Earth Planet Sci Lett 214:499–513

Staudacher T, Allegre C (1988) Recycling of oceanic crust and sediments: the noble gas subduction barrier. Earth Planet Sci Lett 89:173–183

Stevenson DS, Blake S (1998) Modeling the dynamics and thermodynamics of volcanic degassing. Bull Volcanol 60:307–317

Taran YA (1986) Gas geothermometers for hydrothermal systems. Geochem Int 27:111–126

Taran YA (1988) Geothermal gas geochemistry. Nauka, Moscow, in Russian

Taran YA (1992) Chemical and isotopic composition of fumarolic gases from Kamchatka and Kuril islands. Rep Geol Surv Japan 279:183–187

Taran YA (2009) Geochemistry of volcanic and hydrothermal fluids and volatile budget of the Kamchatka-Kuril subduction zone. Geochim Cosmochim Acta 74:1128–1157

Taran YA (2011) N_2, Ar, and He as a tool for discriminating sources of volcanic fluids with application to Vulcano, Italy. Bull Volcanol. doi:10.1007/s00445-011-0448-1

Taran YA, Giggenbach WF (2003) Geochemistry of light hydrocarbons in volcanic and hydrothermal fluids. Soc Econ Geol Spec Pub 10:61–74

Taran YA, Giggenbach WF (2004) Evidence for metastable equilibrium between hydrocarbons in volcanic gases. In: Wanty and Seal II (eds) Water-Rock Interaction, pp 193–195

Taran YA, Pilipenko VP, Rozhkov AM (1986) Geochemistry of hydrothermal solutions and gases of the Mutnovsky geothermal system. In: Sugrobov VM (ed) Geothermical and geochemical studies of high-temperature hydrothermal systems. Nauka, Moscow, pp 140–189 (In Russian)

Taran YA, Esikov AD, Cheshko AL (1987) Deuterium and oxygen-18 in waters of the Mutnovsky geothermal region, Kamchatka. Geochem Int 4:458–468

Taran YA, Pokrovsky BG, Doubik YM (1989) Isotopic composition and origin of water in andesitic magmas. Doklady Earth Sci 304:1191–1194

Taran YA, Pilipenko VP, Rozhkov AM, Vakin EA (1992) A geochemical model for fumaroles of the Mutnovsky volcano, Kamchatka, USSR. J Volcanol Geotherm Res 49:269–283

Taran YA, Hedenquist JW, Korzhinsky MA, Tkachenko SI, Shmulovich KI (1995) Geochemistry of magmatic gases of Kudryavy volcano, Iturup, Kuril islands. Geochim Cosmochim Acta 59: 1741–1761

Taran YA, Gavilanes JC, Cortes A (2002) Chemical and isotopic composition of fumarolic gases and the SO_2 flux from Volcan de Colima, Mexico, between the 1994 and 1998 eruptions. J Volcanol Geotherm Res 117:105–119

Taylor BE (1986) Magmatic volatiles: isotopic variation of C, H and S. Rev Mineral 16:185–225

Vakin EA, Kirsanov IT, Pronin AA (1966) Active crater of Mutnovsky volcano. Bull Volcanol Stations 40:25–36 (in Russian)

Vakin EA, Kirsanov IT, Kirsanova TP (1976) Thermal fields and hot springs of the Mutnovsky geothermal area. In "Geothermal systems and thermal fields of Kamchatka". Moscow Nauka, pp 85–114 (in Russian)

Varekamp JC, Kreulen R, Poorter RPE, VanBergen MJ (1992) Carbon sources in arc volcanism, with implications for the carbon cycle. Terra Nova 4:363–373

Villemant B, Boudon G (1999) H_2O and halogen (F, Cl, Br) behaviour during shallow magma degassing processes. Earth Planet Sci Lett 168:271–286

Wallace PJ (2005) Volatiles in subduction zone magmas: concentrations and fluxes based on melt inclusions and volcanic gas data. J Volcanol Geotherm Res 140:217–240

Welhan JA (1988) Origins of methane in hydrothermal systems. Chem Geol 71:183–191

Zelenski ME, Ovsyannikov AA, Gavrilenko GM, Seniukov SL (2002) Eruption of the Mutnovsky volcano, Kamchatka, on March 17, 2000. Volcanol Seismiol 6:25–28 (in Russian)